DEUTSCHES ELEKTRONEN-SYNCHROTRON DESY

ELECTROWEAK INTERFERENCE, NEUTRINO ELECTRON SCATTERING

AND RELATED TOPICS

by

Beate Naroska

Deutsches Elektronen-Synchrotron DESY, Hamburg

NOTKESTRASSE 85 · 2 HAMBURG 52

To be sure that your preprints are promptly included in the
HIGH ENERGY PHYSICS INDEX ,
send them to the following address (if possible by air mail) :

DESY
Bibliothek
Notkestrasse 85
2 Hamburg 52
Germany

ELECTROWEAK INTERFERENCE, NEUTRINO
ELECTRON SCATTERING AND RELATED TOPICS

Beate Naroska

DESY
Notkestr. 85
D-2000 Hamburg 52

INTRODUCTION

The main topic of this review will be the measurement of
electroweak interference in e^+e^- interactions. At the end new results
on neutrino electron scattering from a BNL experiment will be described
and a few new results on the structure of charged weak currents will be
given.

Electroweak interference is studied to test ideas about the
unification of electromagnetic and weak forces, which resulted in the
formulation of the "Standard Model", minimal $SU(2) \times U(1)$, by Glashow,
Salam and Weinberg[1]. The first experiment that was able to prove the
existence of the electroweak interference effect was done at the SLAC
linear accelerator by a SLAC-YALE collaboration[2]. It measured the
asymmetry in the scattering of polarized electrons off deuterium. The
classical signature of weak interactions, parity violation, was used to
find the asymmetry which is only of the order of $10^{-4}Q^2$. With a typical
Q^2 of 1 GeV^2 this meant that the asymmetry was approximately 1/100 of
a percent.

Electroweak effects have also been searched for in atomic physics.
They are expected to induce parity violating transitions, which would
normally be forbidden. Due to the very low momentum transfers involved,
the expected effects are very small. The first experiments were done
on Bismuth and Thallium, in which the electroweak effects are expected
to be enhanced due to the high atomic number Z. Nevertheless the
statistical significance of the measurements was low and the results
were conflicting[3]. The theoretical calculations also turned out to be
difficult and gave ambiguous results. In 1982 a six standard deviation
effect was finally established by C. Bouchiat et al., in an experiment
on Cesium[4]. The calculation of the expected effect could be done
reliably enough in this "hydrogen like" atom[5].

Finally electroweak interference was measured in muon quark scattering in an experiment at CERN by the BCDMS collaboration[6]. In this experiment the asymmetry of the cross section of negative and positive muons with opposite polarization was measured. In contrast to the eD experiment the asymmetry is mainly parity conserving. Due to the increased Q^2 of up to 180 GeV^2 the measured asymmetry was already in the percent region.

All these experiments gave results in full agreement with the Standard Model, consistent with one single value of $\sin^2\theta_W$, the world average of which is $\sin^2\theta_W = 0.23$[7]. When large e^+e^- machines became available, (PETRA started operations for physics in Autumn 1978 and PEP in 1980), a new field was opened to test electroweak unification. The Q^2 region probed here extends to 1600 GeV^2 and is timelike. The energy range was high enough to get maybe a glimpse at the propagator effect before the actual discovery of the Z^O which was recently announced[8]. The main question was: would weak coupling constants be the same as at lower Q^2 and would e^+e^- data also confirm the universal validity of the Standard Model? In addition e^+e^- interactions are maybe the only tool for measuring the weak couplings of heavy quarks, such as charm, bottom, and the still elusive top.

The outline of the review is as follows:

1. Notation, electroweak parameters, and basic equations
2. Bhabha scattering
3. $e^+e^- \rightarrow \mu^+\mu^-\gamma$ and $\mu^+\mu^-\gamma\gamma$
4. $e^+e^- \rightarrow \mu^+\mu^-$
5. $e^+e^- \rightarrow \tau^+\tau^-$
6. Higher order corrections to the angular asymmetry
7. Coupling Constants
8. Mass of the Z^O
9. Measurement of heavy quark coupling constants
10. Measurement of $\sigma(\nu_\mu e \rightarrow \nu_\mu e)$
11. New results concerning the structure of charged and neutral currents.

Available Data from PETRA and PEP

PETRA has been running at various centre of mass (cm) energies between 12 and 43 GeV. In the energy regions above 30 GeV many data were collected in the form af a scan in steps of 20-30 MeV. Just before this conference a scan between 40 and 43 GeV was completed. In autumn 1983 another increase in energy up to $\sqrt{s} \sim 45$ GeV is foreseen. The bulk of the data, namely ~ 70 pb^{-1} per experiment were collected around 34.5 GeV.

PEP on the other hand has taken most of its data at a fixed cm energy of $\sqrt{s} = 29$ GeV. At the beginning of 1983 a large increase was made in the luminosity collected per day, which reached 1 pb^{-1}. By the time of the conference experiments had collected up to 150 pb^{-1},

although part of the data have yet to be analysed.

1. THE ELECTROWEAK CROSS SECTION

In this chapter some of the basic equations of electroweak theory will be recapitulated, mainly to introduce notation.

In lowest order of electroweak theory the amplitude for $e^+e^- \to f^+f^-$ is expressed as the sum of the electromagnetic and the weak amplitude:
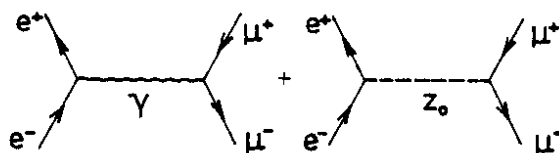
If $f = e$ the t channel must also be taken into account. For the moment we shall restrict the discussion to $f \neq e$. The differential cross section for $e^+e^- \to f^+f^-$, where f can be μ, τ or a quark q, can then be written as[9]:

$$\frac{d\sigma}{d\Omega} = \frac{\alpha^2}{4s} \cdot (C_1 \cdot (1 + \cos^2\theta) + C_2 \cdot \cos\theta) \tag{1}$$

$$\text{with} \quad C_1 = Q_f^2 - 2 \cdot Q_f \cdot v_e v_f \chi + (v_e^2 + a_e^2) \cdot (v_f^2 + a_f^2) \cdot \chi^2$$

$$\text{and} \quad C_2 = -4Q_f \cdot a_e a_f \chi + 8 \cdot v_e v_f a_e a_f \cdot \chi^2.$$

Q_f is the electrical charge of the fermion. a_e, v_e, a_f and v_f denote the vector and axial vector coupling constants of the Z^0 to the electron and final state fermion currents. $\chi = g \cdot s \cdot M_Z^2 / (s - M_Z^2)$ and $g = G_f / (8 \cdot \pi\alpha \cdot \sqrt{2})$ where G_f is the Fermi coupling constant and M_Z the mass of the Z^0.

In (1) we have assumed factorisation, that is the exchange of one neutral boson Z^0 only. The coefficients C_1 and C_2 contain an interference term ($\sim\chi$) and a weak term ($\sim\chi^2$). In C_1 these terms, however, turn out to be negligible at presently available energies as they contain the vector coupling constant of the electron which is close to 0. In the coefficient C_2 on the other hand, the interference term contains only axial coupling constants and therefore becomes sizeable at high s. Neglecting the small purely weak contribution $\sim\chi^2$ in C_2 the integrated asymmetry A is:

$$A = (F-B)/(F+B) = -1.5 \cdot a_e a_f \cdot \chi / Q_f \tag{2}$$

where F and B denote the cross sections integrated over the forward and backward region respectively. The asymmetry depends only on the axial coupling constants of the Z^0 to the fermions and, via the propagator,

on the mass of the Z^0. As the electric charge, Q_f, enters in the denominator, asymmetries are expected to be large for quarks of fractional charge.

The vector coupling constants can only be derived from the absolute value of the cross sections. The smallness of the vector coupling constant of the electron however implies that high precision measurements are required to get good constraints on the vector coupling constants.

The vector and axial vector coupling constants are given by the third component of the left- and right-handed weak isospins $T_L(f)$ and $T_R(f)$ of the fermions:

$$a_f = 2 \cdot \sqrt{\rho} \cdot (T_{3L}(f) - T_{3R}(f))$$

$$v_f = 2 \cdot \sqrt{\rho} \cdot (T_{3L}(f) + T_{3R}(f) - 2 \cdot Q_f \cdot \sin^2\theta_W) \tag{3}$$

The parameter ρ is the relative strength of neutral and charged weak currents, $\rho = M_W^2 / M_Z^2 \cos^2\theta_W$. ρ is predicted to be 1 in the Standard Model and more generally in all models that contain only Higgs doublets. Within the Standard Model the weak isospin is defined and the coupling constants are fixed and depend only on the one free parameter $\sin^2\theta_W$ (see table I).

Using $\sin^2\theta_W = 0.23$ and neglecting mass effects, one predicts the following asymmetries at $\sqrt{s} = 35$ GeV: A = -9.4% for $\mu^+\mu^-$, A = -14% for $c\bar{c}$ and A = -28% for $b\bar{b}$. At $\sqrt{s} = 29$ GeV the corresponding numbers are -6%, -9% and -18%.

Particle f	a_f	v_f	$v_f(\sin^2\theta=0.23)$
e, μ, τ	-1	$-1 + 4 \cdot \sin^2\theta$	-0.08
$u, c, (t)$	+1	$+1 - 8/3 \cdot \sin^2\theta$	0.39
d, s, b	-1	$-1 + 4/3 \cdot \sin^2\theta$	-0.69

Table I.   Weak Coupling Constants in the Standard Model

2. BHABHA SCATTERING

High statistics data for $e^+e^- \rightarrow e^+e^-$ exist from CELLO[10], JADE[11], MARK J[12], and TASSO[13] at PETRA at an average cms energy of $\sqrt{s} = 34.5$ GeV and, from HRS[16], MAC[15] and MARK II[14] at PEP at $\sqrt{s} = 29$ GeV. The differential cross sections are corrected for contributions up to order α^3 using the Monte Carlo programs by Berends and Kleiss[17]. The ratio of the measured
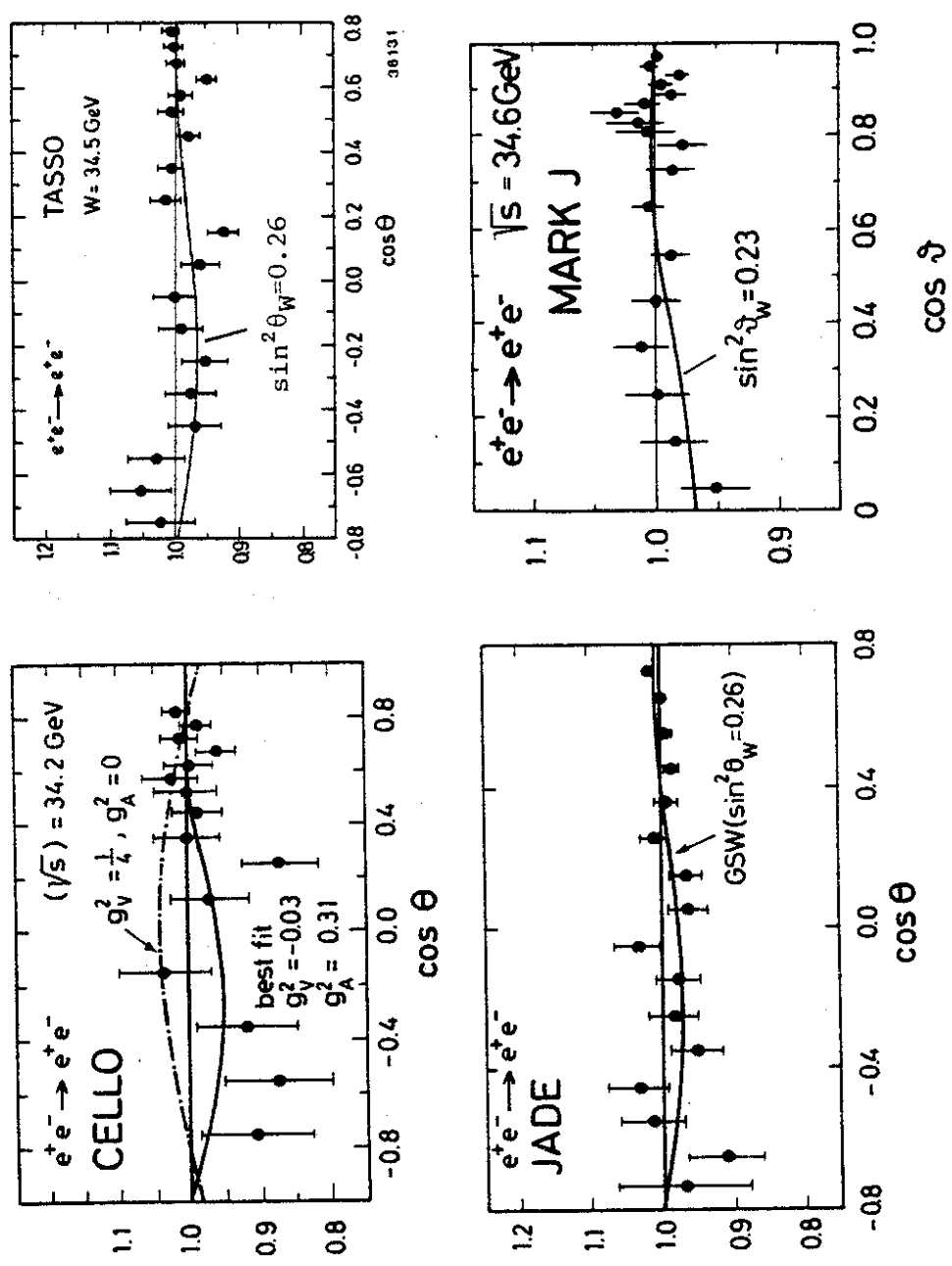
$$\frac{d\sigma}{d\Omega} \Big/ \frac{d\sigma_{QED}}{d\Omega}$$

Fig. 1: The differential cross section for $e^+e^- \to e^+e^-$ divided by the QED expectation for PETRA experiments. The straight line at 1 indicates the QED prediction; the curves deviating from 1 also take into account the electroweak interference.
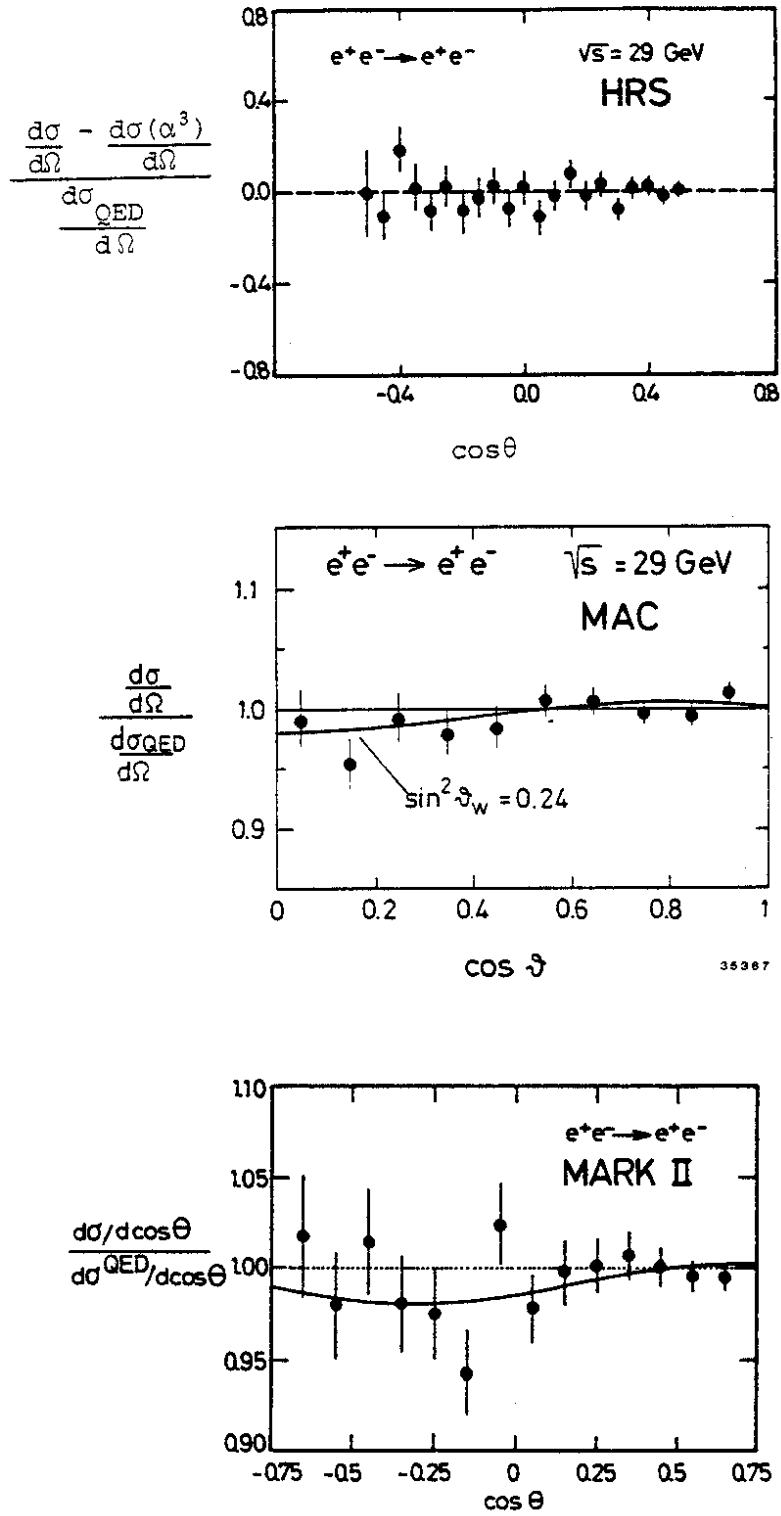
Fig. 2:   Angular distributions for Bhabha scattering for the PEP experiments.

cross section to the QED expectation is displayed in fig. 1 for the PETRA experiments and in fig. 2 for the PEP experiments.(Note that MAC and MARK J do not separate the forward and backward direction!) The data agree well with QED, which is represented by a straight line at 1 (or at 0 for HRS).

The electroweak cross section for $e^+e^- \to e^+e^-$ is complicated due to the presence of the t-channel which reduces the residual deviations from QED considerably. In fig. 3 the expected deviations from QED are shown for several values of $\sin^2\theta_W$. They are only of the order of 2 to 3% for $\sin^2\theta_W$ near 0.25. The fact that the data agree well with QED rules out values of $\sin^2\theta_W$ vastly different from 0.25. The largest deviations from QED occur in the backward direction ($\cos\theta<0$), where the statistical error still dominates in the data. Therefore no experiment has yet been able to claim a significant deviation from pure QED although the χ^2 of the fits tends to get better if the weak effect is included.
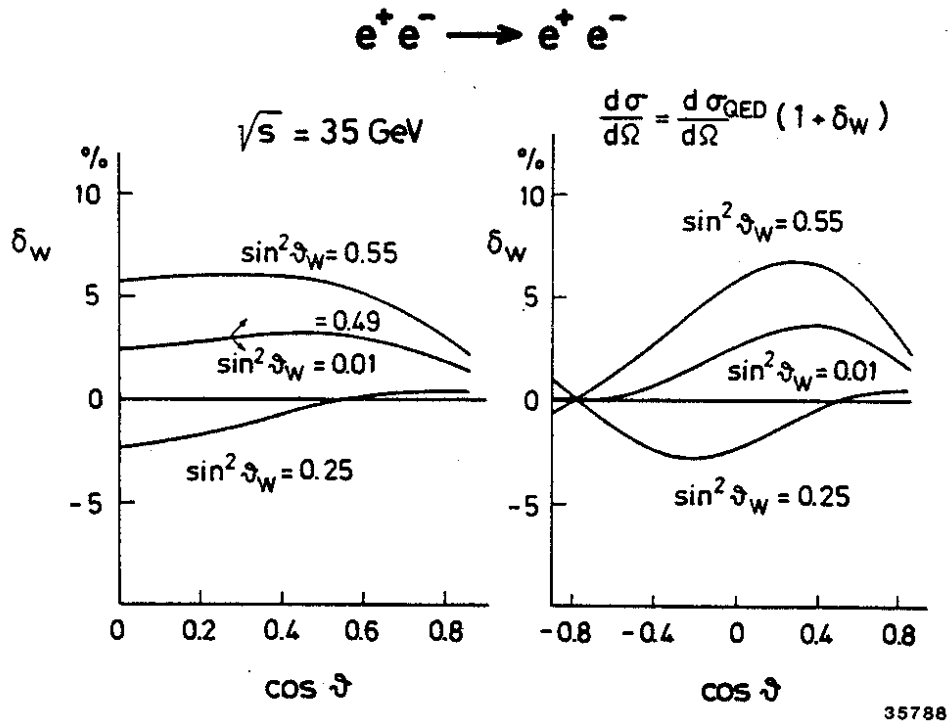

$$e^+e^- \longrightarrow e^+e^-$$

Fig. 3: Deviations expected in Bhabha scattering due to electroweak interference for experiments without and with charge separation.

3. $e^+e^- \to \mu^+\mu^-\gamma$ AND $\mu^+\mu^-\gamma\gamma$

An important correction for the analysis of e^+e^- data, and especially of the angular asymmetry of muon and tau pairs, comes from contributions of higher order in the electromagnetic coupling constant α. These corrections can be calculated within the framework
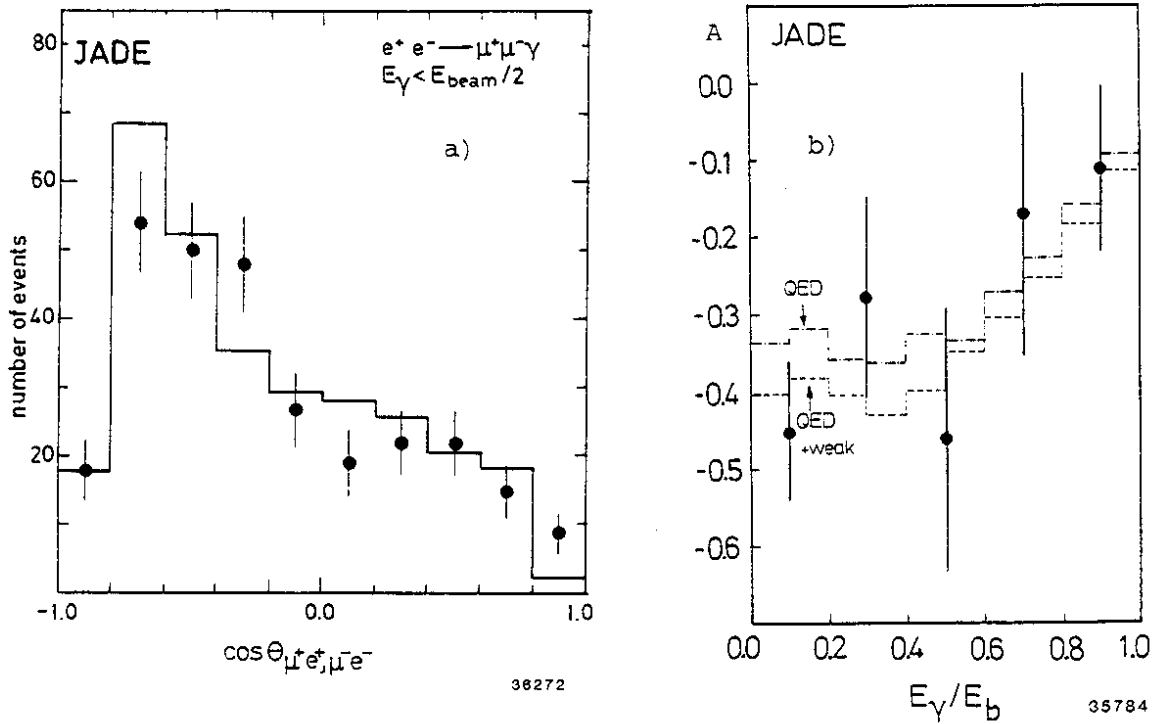
Fig. 4: $e^+e^- \rightarrow \mu\mu\gamma$ from JADE at $\sqrt{s} - 34.2$ GeV. a) Angular distribution. The histogram represents QED to α^3. b) Forward backward asymmetry as a function of the photon energy.
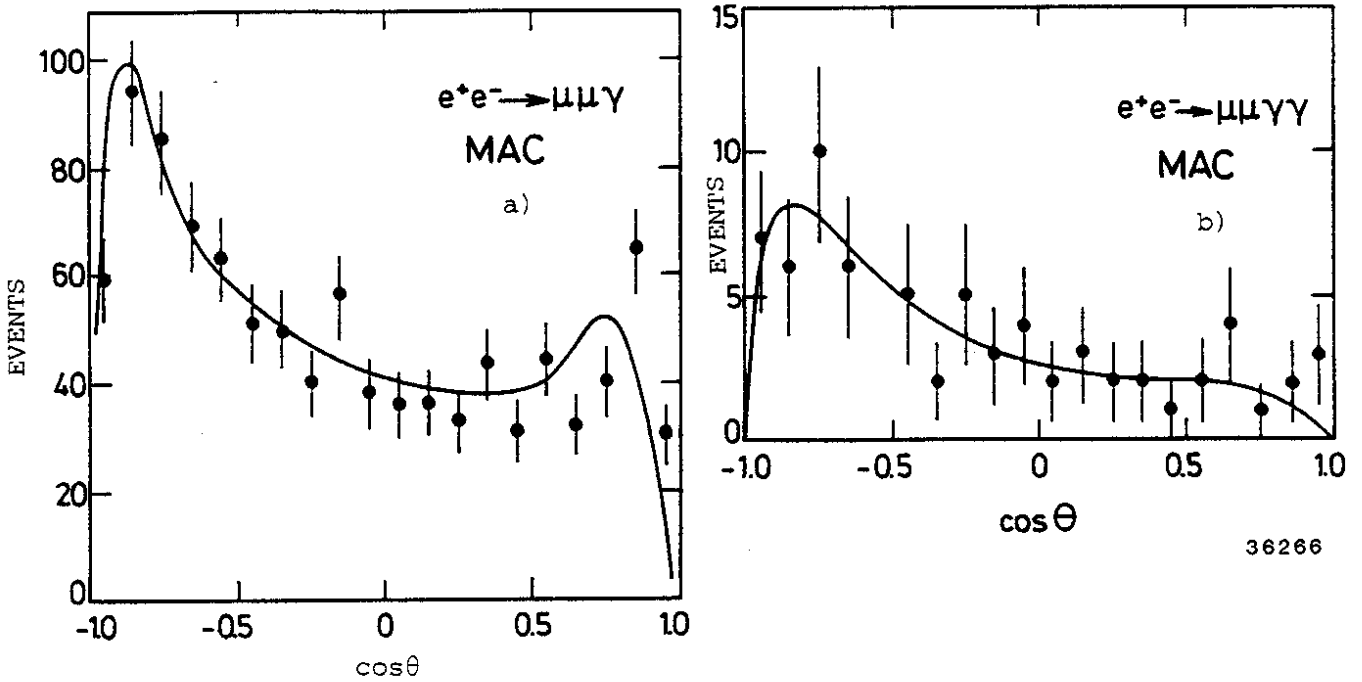

Fig. 5: Angular distribution from MAC for a) $e^+e^- \rightarrow \mu\mu\gamma$ and (b) $e^+e^- \rightarrow \mu\mu\gamma\gamma$. The curves represent the prediction from QED to order α^3 for (a) and α^4 for (b).

of QED and, in general, depend on the experimental cuts applied. Measurements of processes of order α^3 and α^4 have been carried out and provide a possibility to test QED and to check the calculations.

A variety of processes has been measured by the JADE group and found in good agreement with calculations: $e^+e^- \rightarrow e^+e^-\gamma$, $\gamma\gamma\gamma$[11] and $\mu^+\mu^-\gamma$. The angular distribution for $\mu^+\mu^-\gamma$ for photon energies 1 GeV $< E_\gamma < E_{beam}/2$ is shown in fig. 4a as measured by the JADE group. A substantial asymmetry of $-(39 \pm 8)$% is observed in good agreement with the calculations of Berends and Kleiss which give $-(34 \pm 0.6)$%[18]. If the electroweak effect is included one obtains $(-40 \pm 0.6\%)$[19]. The available statistics does not allow one to distinguish the electroweak effect. The asymmetry as a function of the photon energy is shown in fig. 4b.

Similar studies for $\mu^+\mu^-\gamma$ and the α^4 process $e^+e^- \rightarrow \mu^+\mu^-\gamma\gamma$ were done by the MAC group[20]. The angular distributions are displayed in fig. 5a and b. The calculation of the latter process was done by Rek and Schmitt[21]. MAC finds, using all photon energies > 1 GeV in $e^+e^- \rightarrow \mu\mu\gamma$ an asymmetry of (-21.7 ± 3.1)%, whereas they expect (-21.1 ± 1.3)% from QED. In $e^+e^- \rightarrow \mu\mu\gamma\gamma$ they find A = (-37 ± 11)% and expect (-36.4 ± 4.8)%. The weak effect, which is calculated to be -2% under their experimental conditions, is not included in the expected values.

4. $e^+e^- \rightarrow \mu^+\mu^-$

This is the gold plated reaction in e^+e^- physics in which the existence of the forward backward asymmetry could be first demonstrated[22]. Since the first observation of the muon asymmetry, statistics have improved. The experiments JADE, MARK J and TASSO at PETRA have $\sim$3000 events each at an average cm energy of $\sqrt{s}$ of 34.5 GeV and CELLO and PLUTO somewhat less as they shared one interaction region[23]. In addition smaller amounts of data are available at low cm energies and first new preliminary data at a cm energy of $\sim$40 GeV. At PEP at a cm energy of 29 GeV the MAC experiment was the first to get more than 10000 events[24]. MARK II has analysed $\sim$5300[14], and HRS $\sim$1000 μ pairs[16].

The signature of events is simple: two high momentum, minimum ionizing, penetrating particles, emerging almost back to back from the beam intersection. Typical experimental requirements are more than half the beam momentum for each muon, and an acollinearity angle below 10°. Possible background from cosmic rays and Bhabha scattering can be kept at a negligible level. Contributions from two photon μ pair production and τ decays are at the percent level and are easily calculable.

The data from all groups except MARK II are corrected for QED contributions up to order α^3, utilizing programs by Berends and Kleiss[18] (see also chapter 6 on higher orders).
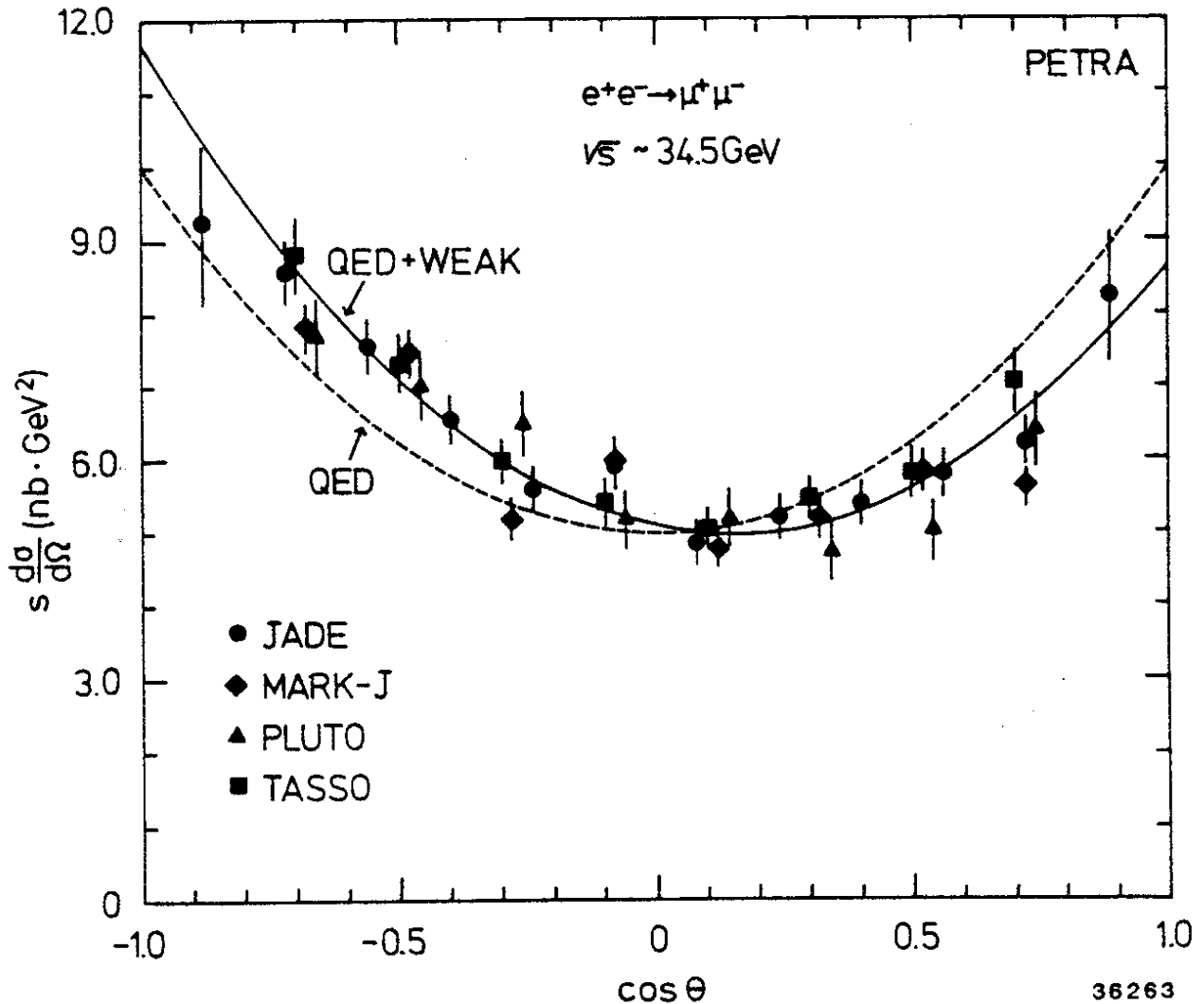
Fig. 6: Angular distributions for $e^+e^- \rightarrow \mu^+\mu^-$ for JADE, MARK J, PLUTO and
TASSO at $\sqrt{s}$ 34.5 GeV. The data are corrected for QED effects up
to α^3. The full curve shows a fit to the data allowing for an
asymmetry, the dashed curve is the symmetric QED prediction.

The angular distributions of the 4 high statistics PETRA
experiments are compiled in fig. 6. The data agree well with each other.
Similar distributions for three PEP experiments are shown in
fig. 7. In all histograms the full curve represents a fit of the
data to the electroweak cross section (1). The dashed curve gives the
prediction of QED in lowest order (except for MARK II, where it is to
order α^3). Clear systematic deviations from pure QED are seen for all
experiments.

The asymmetries for the full angular range derived from the fits
to the data are listed in table II together with the expectation from
the lowest order electroweak theory with $a_e \cdot a_\mu = 1$ and $M_Z = 90$ GeV.
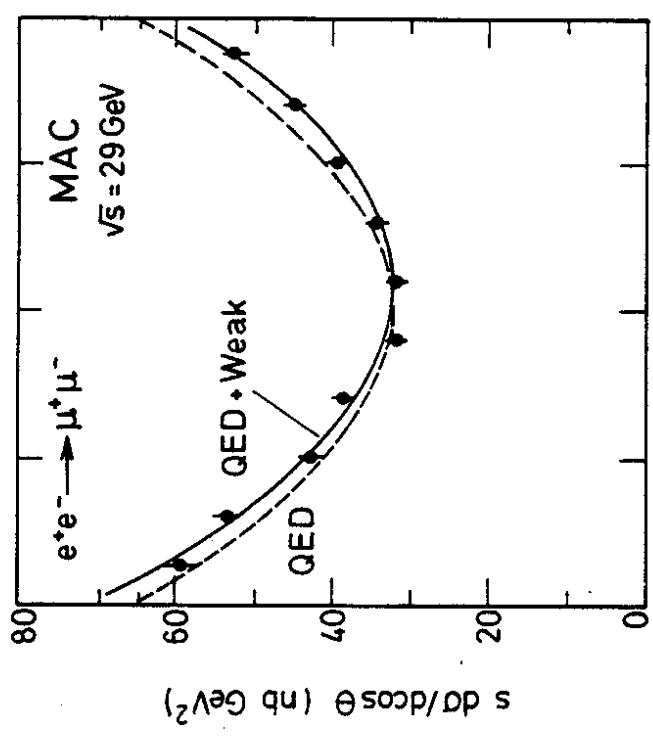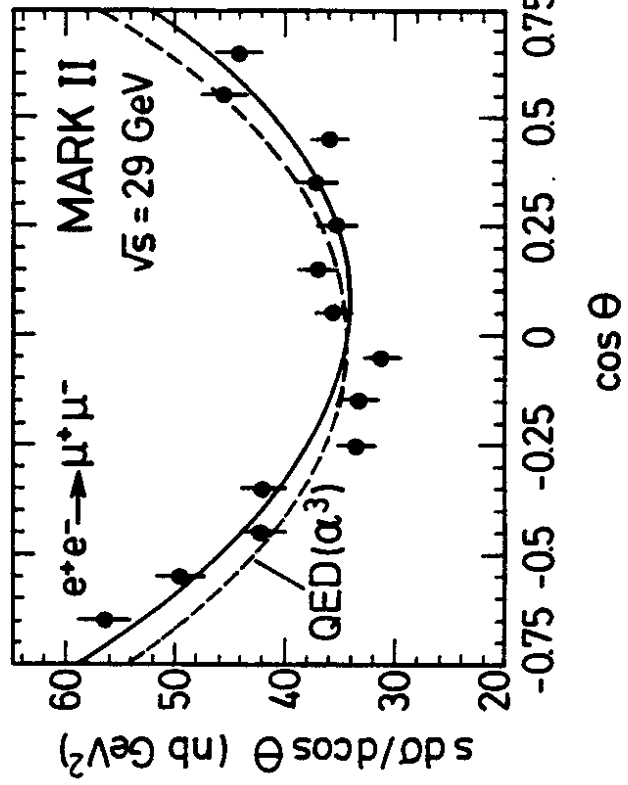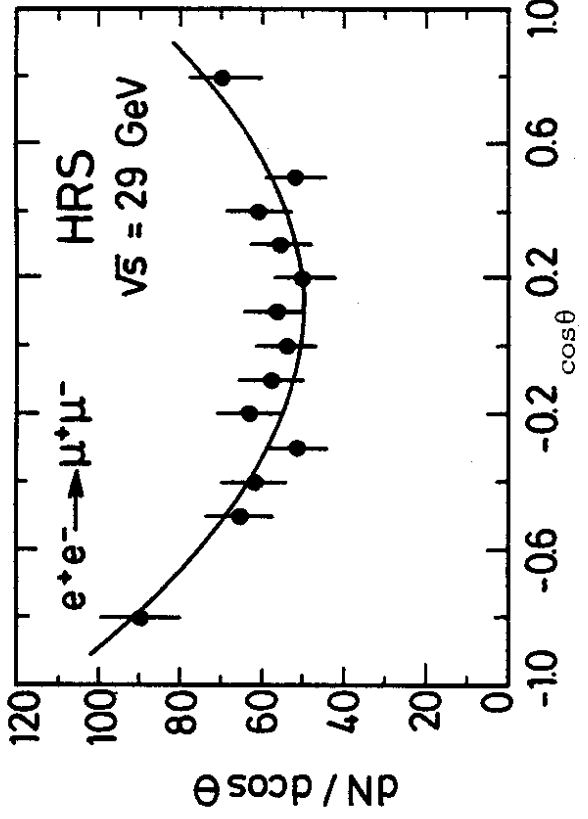When two errors are shown the first one is statistical and the second

Fig. 7: Angular distributions for $e^+e^- \rightarrow \mu^+\mu^-$ for HRS, MAC and MARK II at $\sqrt{s}$ = 29 GeV. The data of HRS and MAC are corrected for α^3 effects. The full curve shows a fit to the data allowing for an asymmetry; the dashed curve is the symmetric QED prediction (for MARK II it shows QED to order α^3).

36271

EXP	$\sqrt{s}$ |GeV|	$\int L dt$ |pb^{-1}|	$N_{\mu\mu}$	$A_{\mu\mu}$ |%|	A_{GWS} |%|
HRS	29	20	979	-8.4 ± 4.3	
MAC	29	143	10258	$-5.8 \pm 1.0 \pm 0.3$	-6.3
MARK II	29	100	5312	-7.1 ± 1.7	
AVERAGE	29	263	16549	-6.3 ± 0.9	6.3
CELLO	34.2	11.3	387	-6.4 ± 6.4	-9.2
JADE	34.4	71.2	3400	$-11.0 \pm 1.8 \pm (<1)$	-9.3
MARK J	34.6	76.3	3658	$-11.7 \pm 1.7 \pm (<1)$	-9.5
PLUTO	34.7	44	1550	$-12.4 \pm 3.1 \pm (<1)$	-9.5
TASSO	34.5	74.7	2673	$-9.1 \pm 2.3 \pm 0.5$	-9.4
AVERAGE	34.5	277.5	11668	-10.8 ± 1.1	-9.4
JADE	40.3	8.2	325	-13.3 ± 6.0	-13.6
MARK J	39.5	8.1	210	-11.3 ± 6.9	-13.0
TASSO	41.2	5.2	99	-11.4 ± 10.0	-14.5
AVERAGE	40.2	21.5	634	-12.3 ± 4.1	-13.5

Table II: Angular Asymmetries of Muon Pairs

one the estimated systematic error. For the averaged values these have
been added in quadrature. The agreement between measurement and
expectation is good for all experiments. The significance of the
averaged asymmetries amounts to 10 standard deviations both at $\sqrt{s}$ of
29 and 34.5 GeV. The last values in table II come from the most
recent data at PETRA at $\sqrt{s}$ around 40 GeV. They also agree with
expectations but should still be considered as preliminary.

$$5. \quad e^+e^- \rightarrow \tau^+\tau^-$$

Studies of τ pair production are more complicated due to the decay
of the τ which results partly in electrons and pions that have a large
probability of interacting in the material of the detector and partly
in neutrinos that escape unseen altogether. The signature of events
is therefore much more ambiguous, thereby decreasing the detection
efficiency. Backgrounds can come from many more sources than in the
muon final state, but in general they are calculable and can be kept at

the level of a few percent. In general not all decay modes are used by the groups and this further reduces statistics. New data are available from JADE and MARK J at PETRA and from MARK II at PEP. All available PETRA data [25] at $\sqrt{s} \sim 34.5$ GeV are shown in fig. 8. The MARK II data [14] are shown in fig. 9.
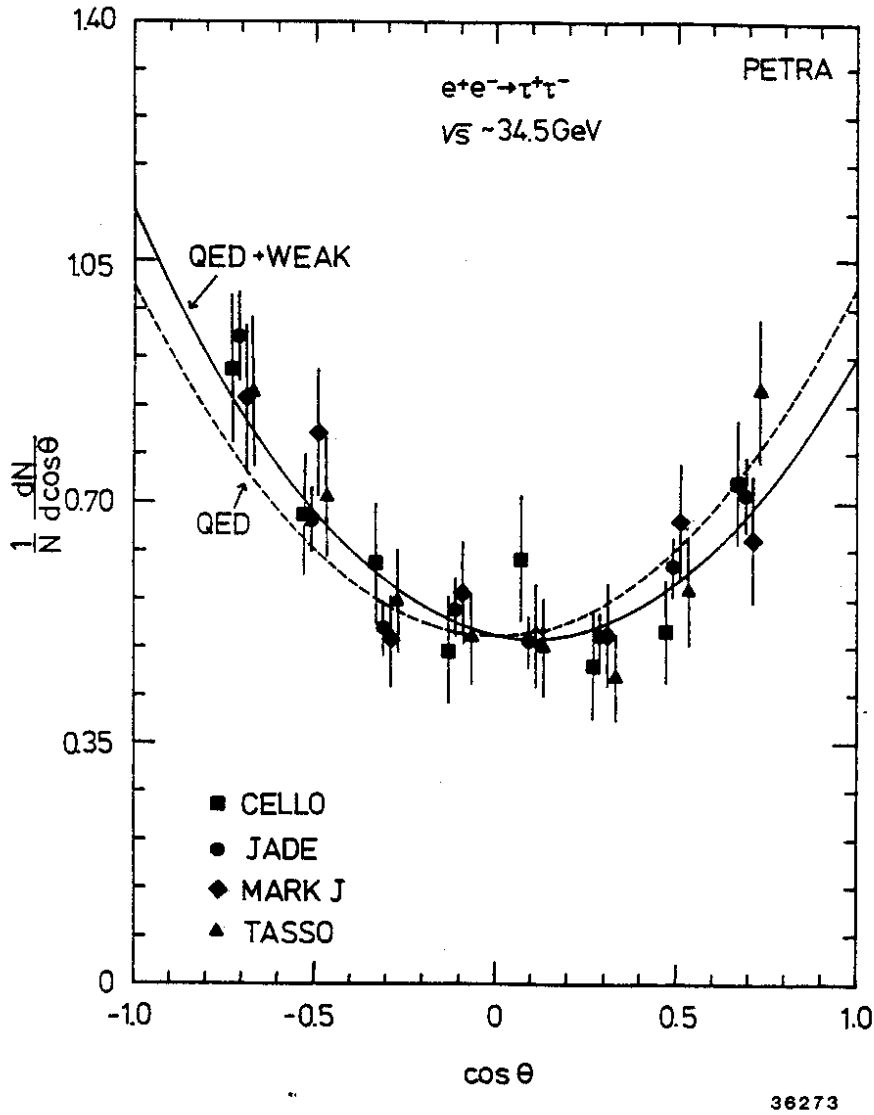

Fig. 8: Angular distribution for $e^+e^- \rightarrow \tau^+\tau^-$ for CELLO, JADE, MARK J, and TASSO at $\sqrt{s} \sim 34.5$ GeV, corrected for QED effects up to α^3. The full curve shows a fit to the data allowing for an asymmetry, the dashed curve is the symmetric QED prediction.
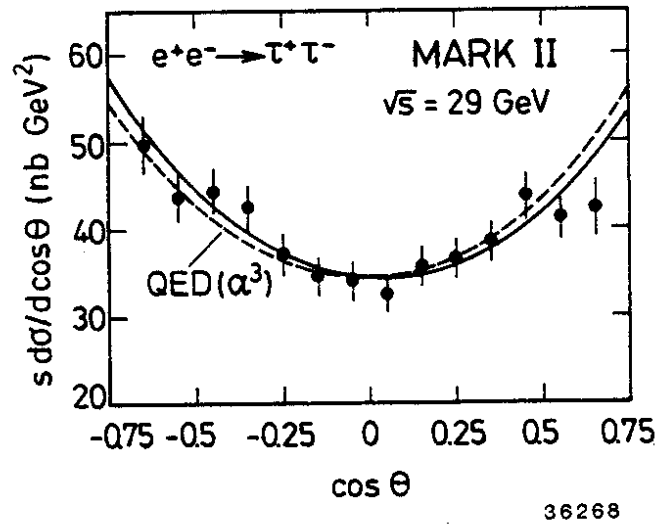
36268

Fig. 9: Angular distributions for $e^+e^- \to \tau^+\tau^-$ for MARK II. The full
curve shows a fit to the data allowing for an asymmetry;
the dashed curve is the QED prediction to order α^3.

| EXP	$\sqrt{s}\,|\text{GeV}|$	$\int L\,dt\,|\text{pb}^{-1}|$	$N_{\tau\tau}$	$A_{\tau\tau}\,|\%|$	$A_{GWS}\,|\%|$
MAC	29	30	1247	-1.3 ± 2.9	$\left.\begin{array}{c}\\\\\end{array}\right\}$ -6.3
MARK II	29	100	3714	-4.2 ± 2.0	
AVERAGE	29	130	4961	-3.6 ± 2.1	
CELLO	34.2	17	434	-10.3 ± 5.2	-9.2
JADE	34.6	70	1612	-7.6 ± 2.7	-9.5
MARK J	34.6	85	860	-7.8 ± 4.0	-9.5
TASSO	34.4	66	517	-5.4 ± 4.5	-9.3
AVERAGE	34.5	238	3423	-7.6 ± 1.9	-9.4

Table III: Angular Asymmetries of τ pairs

The data are again corrected for QED contributions up to order α^3,
except the MARK II data. The results of the fitted asymmetries are
given in table III for the most recent data available from each group.
The errors are larger than for the muon asymmetries, mainly because of
smaller statistics and slightly larger corrections. Within errors, the
agreement between theory and experiments is good. The averaged data

show asymmetries that are 1.5 and 4 standard deviations from 0 at $\sqrt{s} = 29$ GeV and 34.5 GeV respectively. It is interesting to observe, however, that all experiments except CELLO obtain a τ asymmetry that is lower than their measured μ asymmetry. Unfortunately, the limited accuracy does not allow any conclusion yet. Most probably the decreased asymmetry can be accounted for by experimental problems, e.g. background from Bhabha scattering or possibly two photon processes.

6. HIGHER ORDER CORRECTIONS OF THE ANGULAR ASYMMETRY

An important correction for all cross sections and angular distributions in e^+e^- scattering, which has already been mentioned, comes from the contribution of higher orders. Traditionally, the correction due to diagrams up to order α^3 for the amplitude with the photon propagator:
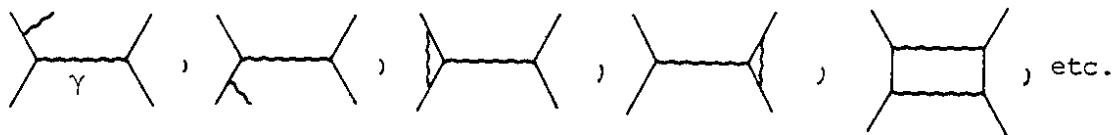
is taken into account in quoting experimental cross sections. The programs by Berends and Kleiss are used[18] to compute the corrections and the data are corrected bin by bin. These corrections which we shall label α^3_γ, lead to an angular asymmetry of +(1 to 2)%; the exact magnitude of which depends on the experimental cuts.

Recently, α^3 contributions to the Z^0 amplitude were also calculated[19], which we shall label α^3_Z. They take into account diagrams where one internal photon has been replaced by a Z^0:
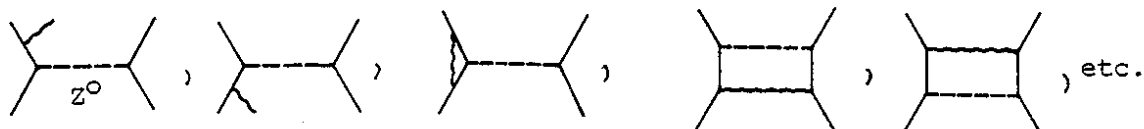
and result in a correction for the measured asymmetry of $\Delta A \sim +0.7\%$ at $\sqrt{s} \sim 34.5$ GeV and $\Delta A \sim +0.3\%$ at $\sqrt{s} = 29$ GeV. This correction has to be subtracted from the measured asymmetry like the α^3_γ correction.

Recently, much effort has gone into calculating higher order contributions in weak interactions (self energy of Z^0, W contributions, Higgs loops, etc.)[27]. Unfortunately, the results are not yet consistent. The correction of the asymmetry ranges from negligible to $\Delta A = -0.6\%$ at $\sqrt{s} = 34.5$ GeV. The latter value would nearly completely cancel the effect of the α^3_Z corrections.

In view of this unsettled situation, we shall compare the measurements corrected for α^3_γ effects, as they are given in tables II and III, to the lowest order electroweak prediction calculated

according to equ. (2). The α^3_z correction and the weak higher orders will be treated as sources of a possible systematic error when computing coupling constants.

7. COUPLING CONSTANTS

7.1 e^+e^- Reactions

The expression (2) for the angular asymmetry depends, besides on the Fermi coupling constant G_f and the mass of the Z^0, only on the axial coupling constants of the electron and the final state fermion. In table IV results for $a_e \cdot a_f$ derived from the averaged asymmetries at $\sqrt{s} = 29$

Data	$a_e a_\mu$	$a_e a_\tau$
PEP	1.00 ± 0.13	0.57 ± 0.33
PETRA	1.12 ± 0.11	0.84 ± 0.20
ALL	1.06 ± 0.09	0.77 ± 0.17

Table IV: Coupling Constants from e^+e^-

and 34.5 GeV are given for μ and τ using a Z^0 mass of 90 GeV. Using $a_e = -1.02 \pm 0.10$ from νe measurements[28] one determines: $a_\mu = -1.04 \pm 0.14$ and $a_\tau = -0.75 \pm 0.18$. Both coupling constants come out to be consistent with -1 and thus confirm e-μ-τ universality, a basic assumption of the Standard Model. If universality is assumed the errors on the axial coupling constants decrease and $|a_\mu| = 1.03 \pm 0.06$ and $|a_\tau| = 0.88 \pm 0.12$ is obtained. The errors given in table IV consist out of statistical and experimental systematic errors. A further systematic error of ~ 0.01 comes from the still uncertain higher order corrections mentioned in chapter 6. It is of the same magnitude as the error due to the uncertainty in the Z^0 mass of roughly ± 5 GeV[8].

7.2 Neutrino Reactions and Comparison to e^+e^-

The weak coupling constants of the electron were first determined in νe scattering experiments. The cross section is very small, so that even the electronic experiments with detectors of several tons target mass have only small numbers of events. Most of the events were collected by two experiments: the CHARM collaboration at CERN measured the cross sections for $\nu_\mu e$ and $\overline{\nu}_\mu e$ scattering[29], while a Virginia-Maryland-Washington-Oxford-Peking collaboration at Fermilab measured only the $\nu_\mu e$ cross section[30].

A compilation of all νe data and a common fit to obtain the weak coupling constants of the electron g_V, g_A, and the electroweak mixing angle $\sin^2\theta_W$ has recently been done[28]. (The definition of g_V and g_A

Fig. 11: 95% confidence level contours for g_V and g_A from $e^+e^- \to \mu^+\mu^-$ and $e^+e^- \to e^+e^-$ from JADE, MARK J and TASSO (shaded area). The open areas are the 95% conf. level contours from a common fit to all νe data. Indicated is also the prediction of the Standard Model.
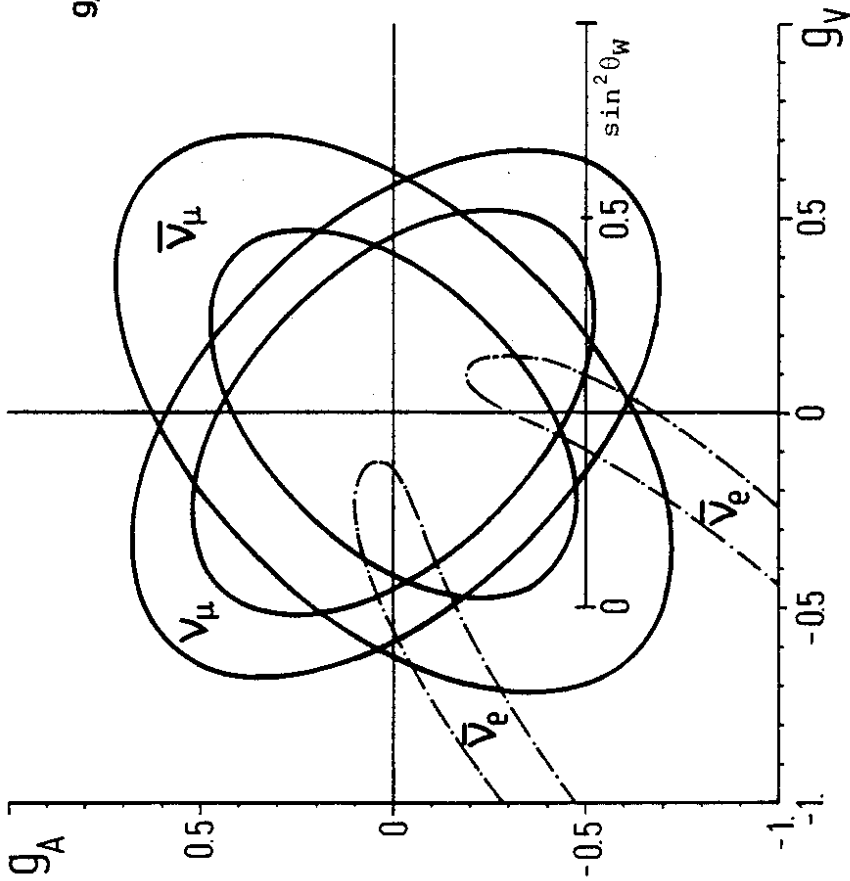

Fig. 10: 90% confidence level contours for g_V and g_A from $\nu_\mu e$, $\bar\nu_\mu e$ and ν_e scattering, all fitted separately.
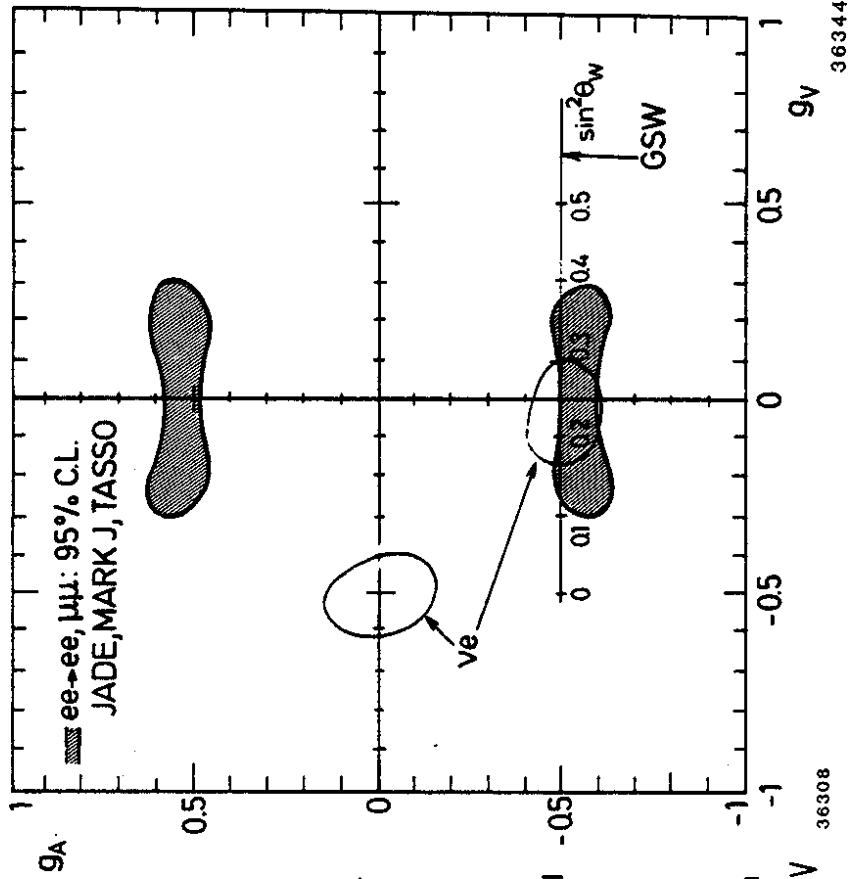
which are commonly used in ν scattering differs by a factor 2 from our v_e and a_e.) In fig. 10 the 90% confidence level contours of the fit to all data on $\nu_\mu e$, $\bar{\nu}_\mu e$, and $\nu_e e$ scattering are displayed. The four-fold ambiguity of ν_μ and $\bar{\nu}_\mu$ scattering is reduced to two overlap regions by also using the reactor data on ν_e scattering.

The two overlap regions give the following values:

1) $g_A = -0.514 \pm 0.058$; $g_V = -0.030 \pm 0.077$ "Axial dominant"

2) $g_A = 0.010 \pm 0.060$; $g_V = -0.526 \pm 0.078$ "Vector dominant"

The 95% confidence level contours of these two solutions are repeated in fig. 11 together with the 95% confidence level contours of a combined fit to $e^+e^- \to e^+e^-$ and $\mu^+\mu^-$ data from JADE, MARK J, and TASSO. This fit, of course, assumes universality. The data from Bhabha scattering are added to give a better constraint on the vector coupling constant.

The axial dominant solution 1) then remains as the only one, consistent with all experiments[31].

7.3 Determination of the Weak Isospin of the Muon

Using expression (3) and the measurement of $T_{3R}(\mu) = 0.00 \pm 0.06 \pm 0.08$ from the BCDMS group[5], the third component of the left handed weak isospin of the muon can be determined from the measurement of the axial coupling constant. We shall assume $\rho = 1$ as predicted by the Standard Model. This is supported by all measurements from neutrino interactions[32], and recently also from direct production of the Z^0[8] and $W^\pm$[8]. We then find $T_{3L}(\mu) = -0.54 \pm 0.08$ from $e^+e^- \to \mu^+\mu^-$ data, in agreement with the standard weak isospin assignment.

8. MASS OF THE Z^0

In fig.s 12 and 13, all available data[33] on the μ and τ asymmetries are plotted as a function of s. For comparison the following curves are shown: a line at A = 0 represents QED or no electroweak effect, which is clearly ruled out by the data. The other curves show the electroweak predictions for different masses of the Z^0 (M = ∞, 90 and 70 GeV) assuming $a_e = a_\mu = a_\tau = -1$.

In order to determine quantitatively limits for the Z^0 mass, the quantity $\chi^2 = \Sigma |A_i - A_i^{exp}|^2 / \sigma_{Ai}^2$ was used. The A_i are the measured asymmetries with error σ_{Ai}, the A_i^{exp} are the expected values calculated according to equation (2). χ^2 is shown as a function of the Z^0 mass in fig. 14. The limits at 95% confidence level for all data are $61 < M_Z < 170$ GeV ($60 < M_Z < 185$ for the PETRA data alone) in full agreement with recent measurements from the UA1 and UA2 collaborations, which give values around 90-95 GeV.
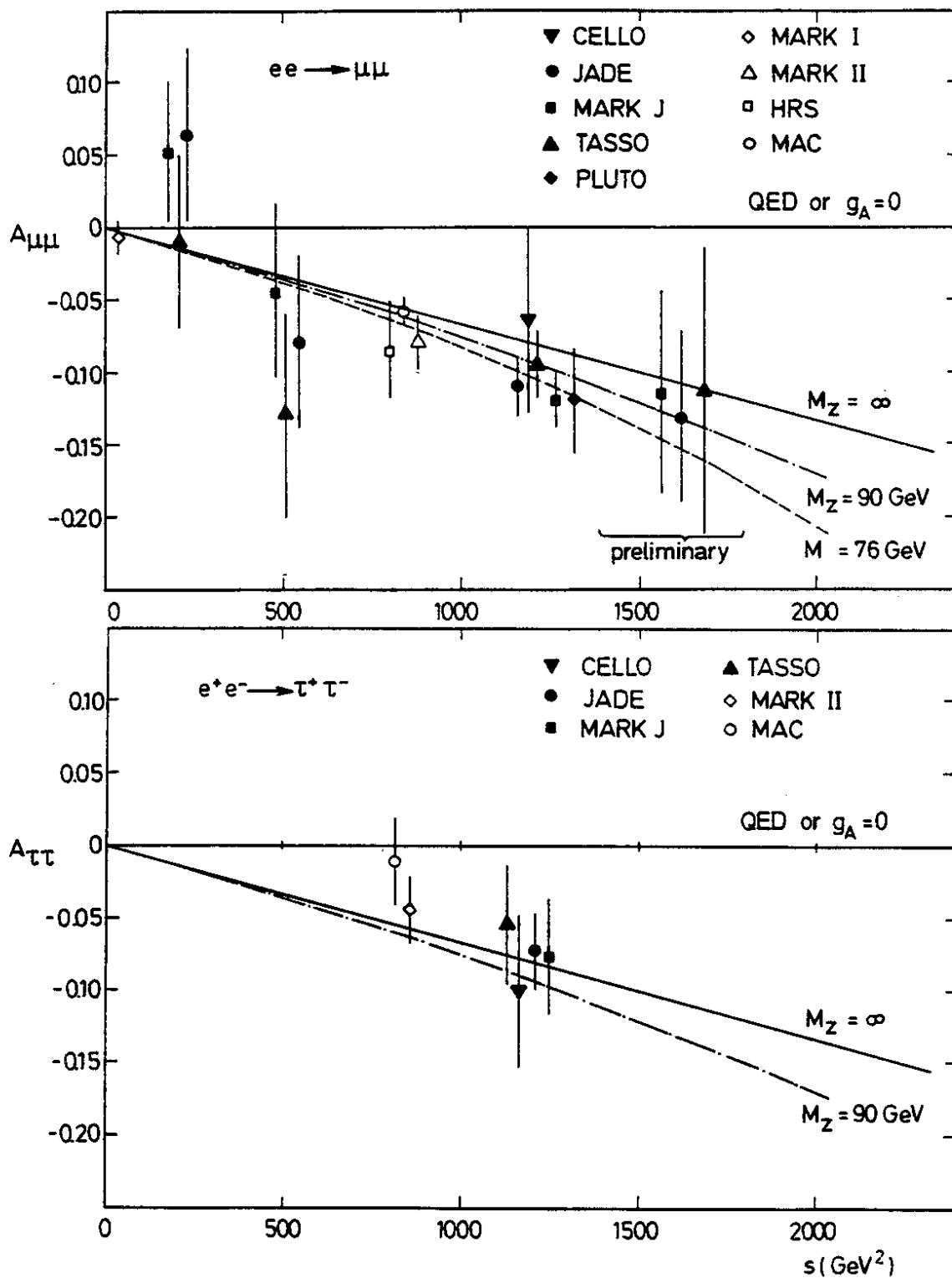
Figs. 12 and 13: The angular asymmetry of $e^+e^- \to \mu^+\mu^-$ and $e^+e^- \to \tau^+\tau^-$ as a function of s. The horizontal line represents pure QED or no electroweak effect. The curves are predictions from the Standard Model with different masses of the Z^0.
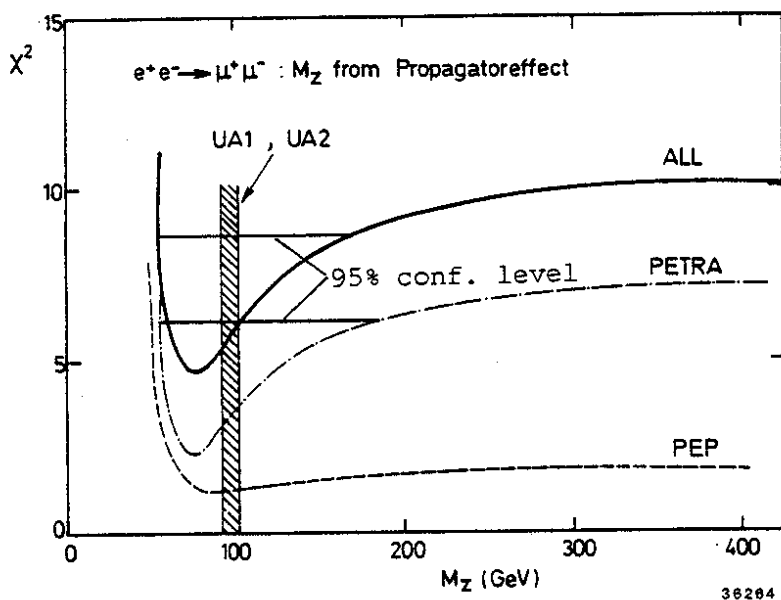
Fig. 14:

Constraints on the mass
of the Z^0 from the propa-
gator effect. For the
definition of χ^2 see text.
The full line includes
all data, the dashed line
all data below $\sqrt{s}$=30 GeV
and the dash-dotted line
is for data above 34 GeV.

9. MEASUREMENT OF HEAVY QUARK COUPLING CONSTANTS

First attempts to determine the weak coupling constants of heavy
quarks in e^+e^- collisions were reported in last summer's conferences[3].
Due to the fractional charge of quarks, one expects asymmetries for the c and
b quark which are roughly a factor 1.5 and 3 larger than for muon
pairs (equ. (2) in chapter 2). The problem is to identify the 4/11 or
1/11 of all multihadronic events that come from primary c and b quarks
respectively. The most promising methods are to identify D or D*
exclusive decays in order to tag c quarks, and to look for the semi-
leptonic decay of c or b. Both methods have a low efficiency mainly
because of the small branching ratios involved. In the search for
inclusive leptons there is in addition a severe background problem.

9.1 Semileptonic Decays of Heavy Quarks

A search for semileptonic decays of heavy quarks is reported by
MAC and MARK II[34] at PEP and by CELLO, JADE, MARK J and TASSO[35,36] at
PETRA. The main handle to separate heavy quarks from the background of
u, d and s induced events is the transverse momentum p_t of the final
state lepton[37]. Thrust or the main axis Q_1 of the normalized momentum
tensor is normally used as reference axis. As an example, the p_t distri-
bution of inclusive muons from the MARK J group is shown in fig.15. To-
gether with the data, two simulated p_t distributions for muons from c
and b decays are shown which indicate a clear difference between b and
c induced events. Adding the b and c contributions and taking into
account the background from punchthrough and decay in flight of pions
and kaons, yields the upper histogram in fig. 15, which fits the data well.

From fig. 15 one can also get a qualitative idea of the background
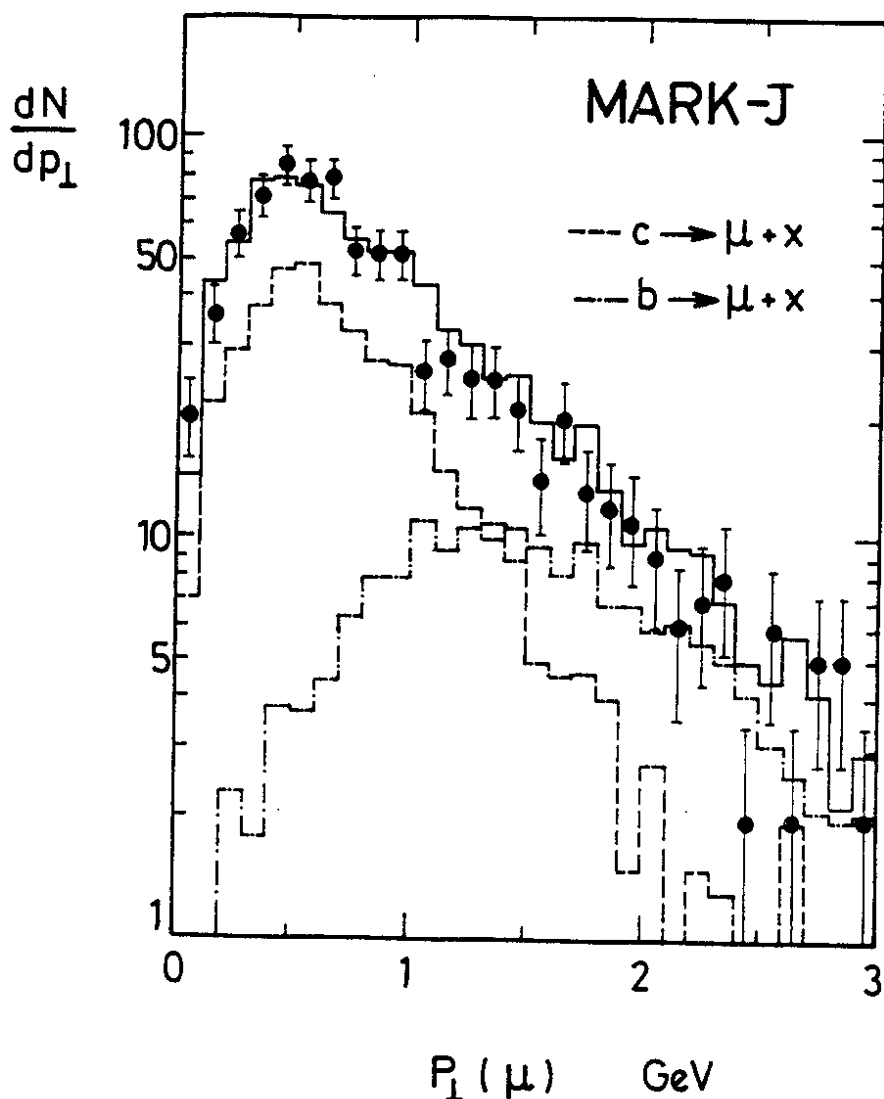
36087

Fig. 15: p_t distributions for inclusive muons from MARK J at $\sqrt{s}$ = 34.5 GeV. Monte Carlo predictions for the contributions from c (dashed) and b (dot-dashed) are shown. The full histogram shows the sum of the two and includes also the background.

which reduces the sensitivity to the heavy quark asymmetry. In the low p_t region, where the c quark dominates over the b, background from u, d and s is abundant. In the high p_t region, where the majority of leptons comes from b decays, c decays which have the opposite asymmetry, are nevertheless still sizeable.

In order to improve the signal to noise ratio, all groups have used a second variable. The MARK II group at PEP and TASSO at PETRA have used the total momentum of the lepton under consideration. MARK II has used both muons and electrons to improve statistics and separated the

events into 3 groups: one which is b enhanced (high p_t and high p), one
that is c enhanced (high p but lower p_t) and a third region which comes
mainly from u, d and s quarks (low p and p_t). The angular distributions
of the inclusive e and μ in these three regions are shown in figs.
16a-c. Best fits to the data (full curves and symmetric predictions
(dashed) are also shown. In the distribution of the b enhanced region
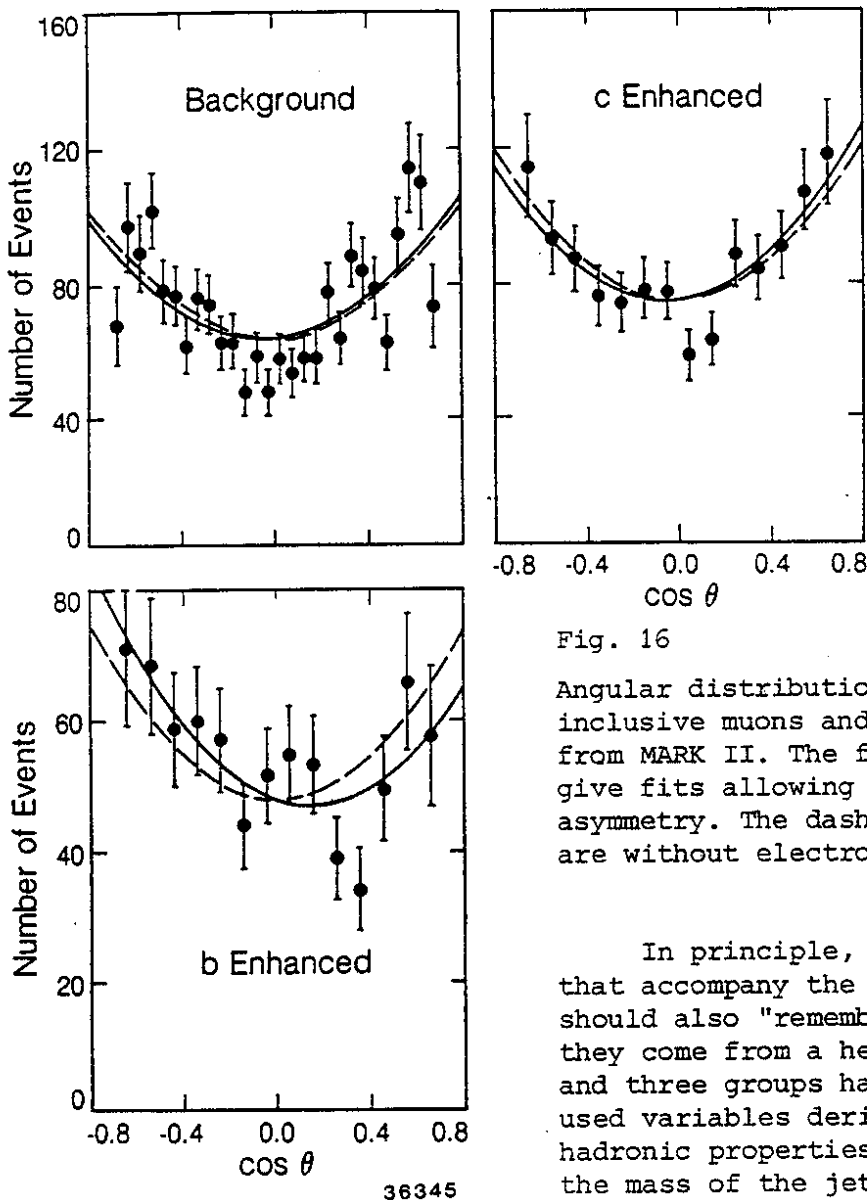the clearest deviation from a symmetric curve is seen.

MARK II

Fig. 16

Angular distributions of
inclusive muons and electrons
from MARK II. The full lines
give fits allowing for an
asymmetry. The dashed lines
are without electroweak effect.

In principle, the hadrons
that accompany the decay lepton
should also "remember" that
they come from a heavy object
and three groups have therefore
used variables derived from
hadronic properties. MAC used
the mass of the jet opposite
to the lepton, JADE used

$\Sigma|p_t|/\Sigma|p|$, where the sum runs over all hadrons in the event, and
MARK J used thrust.
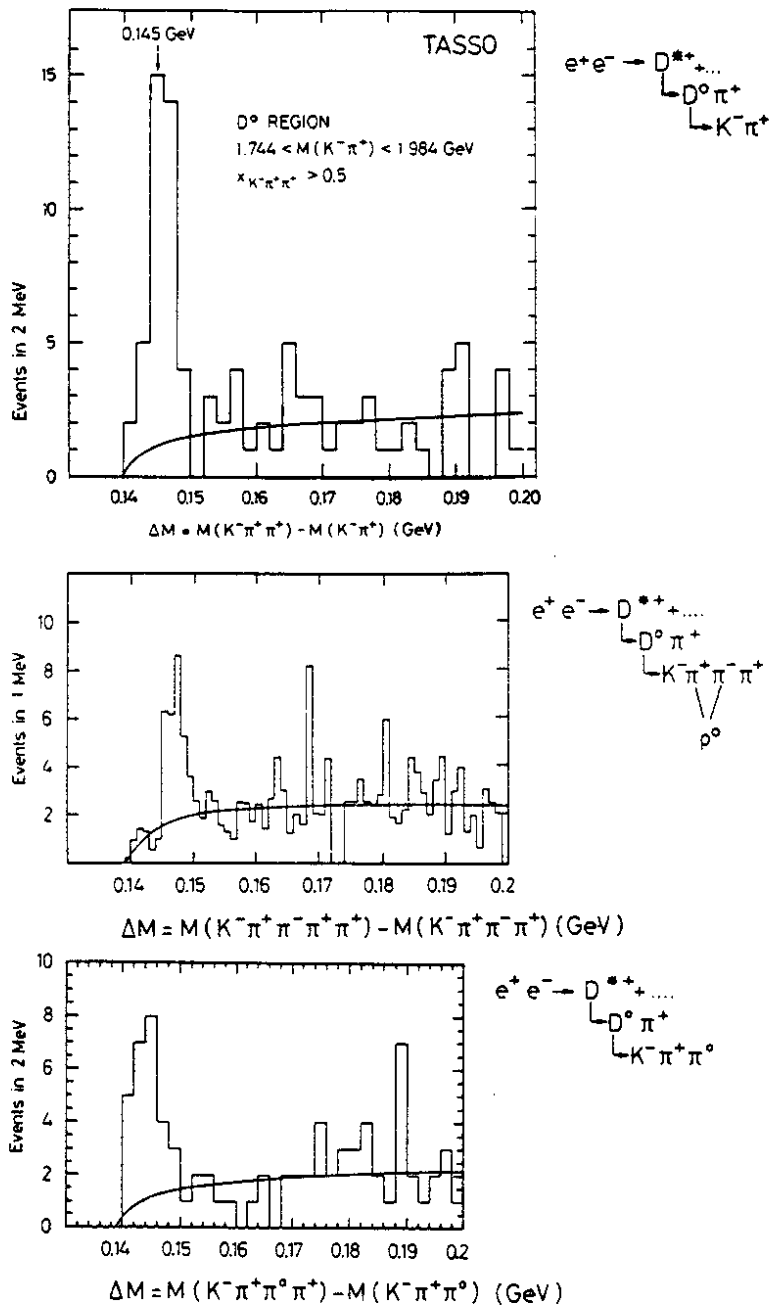
Fig. 17: TASSO D* reconstruction:
ΔM for 3 final states

The asymmetry is usually obtained from fitting the two variables chosen. The results are summarized in table V. Most groups chose to correct their measured asymmetries for background and compared it to the lowest order electroweak prediction. For heavy quarks mass effects are in principle important. They reduce the expected asymmetry[38].
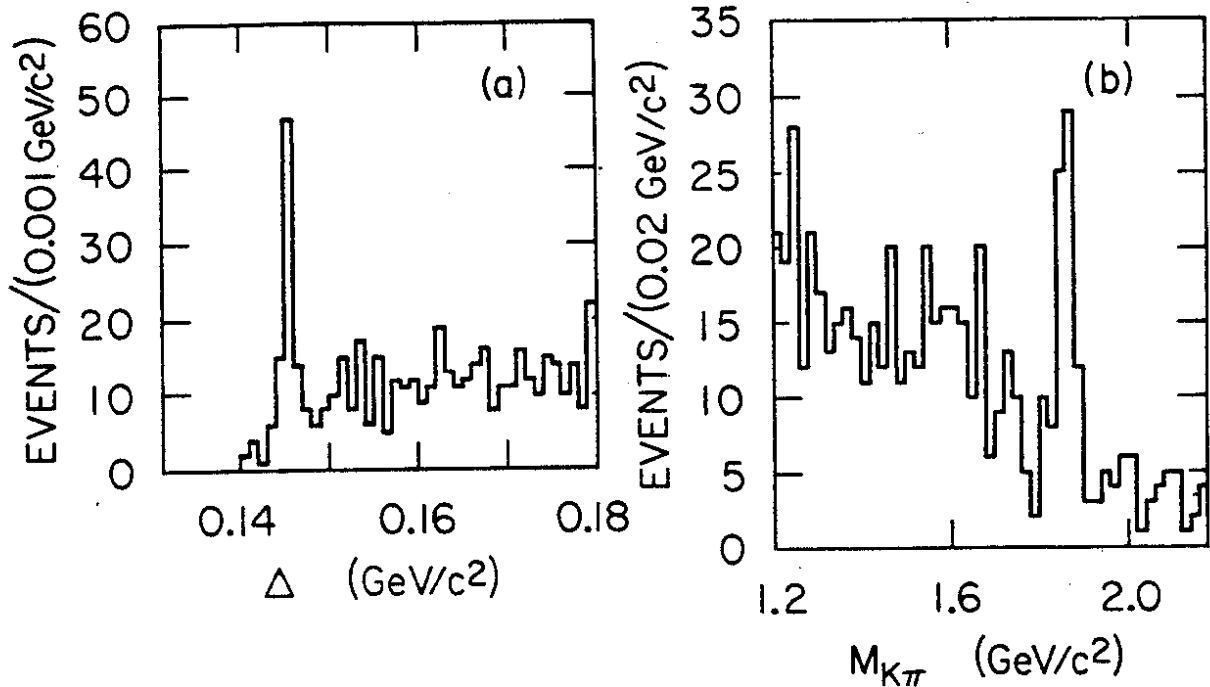
Fig. 18: HRS D* reconstruction in multihadronic events:
a) $\Delta = M(K\pi\pi) - M(K\pi)$, b) $M(K\pi)$

9.2 D* Analysis

Tagging the c quark by reconstructing the D* out of the decay chain:

$$D^{*\pm} \rightarrow D^o \, \pi^{\pm}$$
$$\qquad\qquad \hookrightarrow K^- \, \pi^+$$
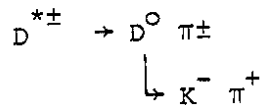
yields a sample of events relatively free of background. This method was used by HRS, JADE and TASSO[39]. No particle identification is used (yet) in order to reduce the combinatorial background. Although, except in the HRS experiment, no signal is seen in the mass of $K\pi$, the D* signal is found by using the well known method of cutting in the mass difference $\Delta = M(K\pi\pi) - M(K\pi)$. Δ shows a peak near 145 MeV for D* decays. TASSO also uses the following decay modes of the D^o in order to increase the statistics:

$$D^o \rightarrow K^- \pi^+ \pi^+ \pi^-$$
$$D^o \rightarrow K^- \pi^+ \pi^o$$
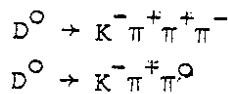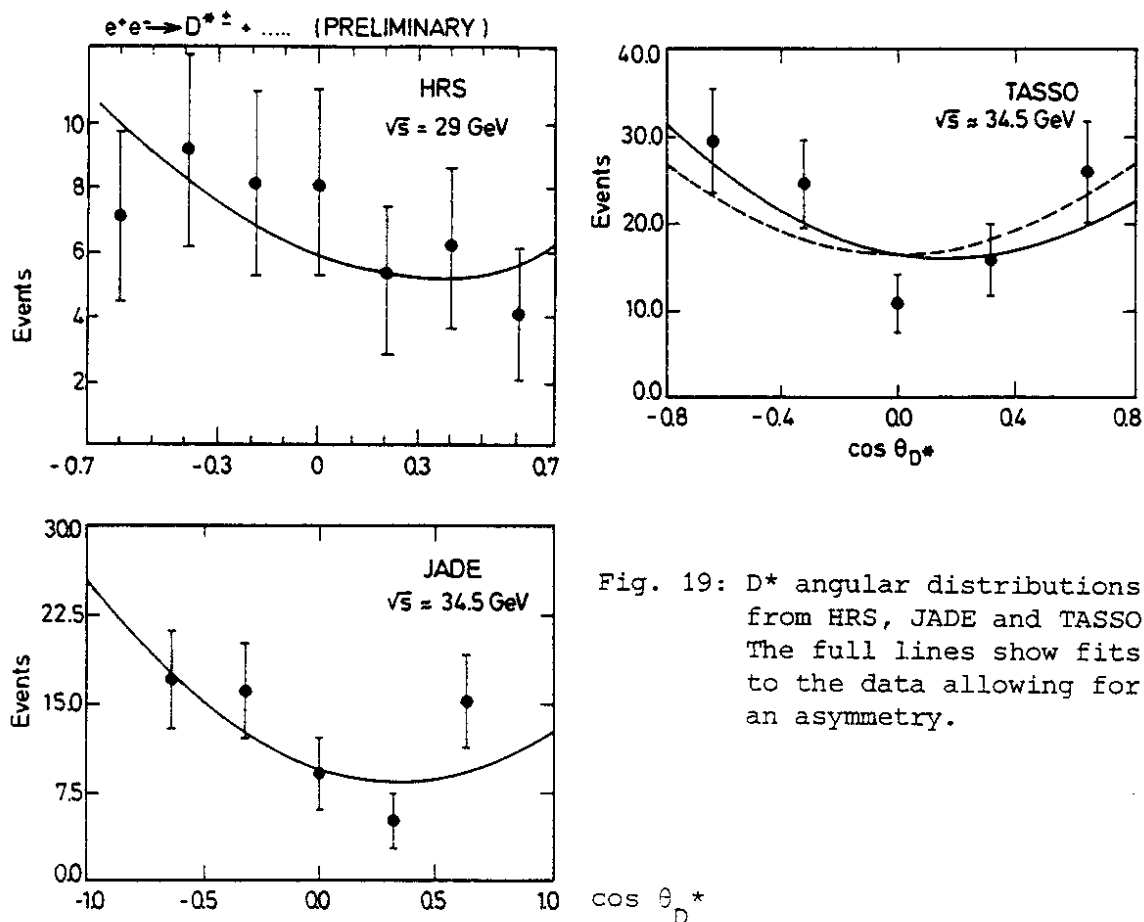
Fig. 19: D* angular distributions from HRS, JADE and TASSO. The full lines show fits to the data allowing for an asymmetry.

The mass differences for the three decay modes used by TASSO are shown in fig. 17.

The HRS, due to their superior momentum resolution of 0.1%·p, can see the D^0 directly and will also use the D^0 to tag the c quark once more statistics are available. The Δ and $K\pi$ mass distribution of HRS are shown in fig. 18.

After the cut in Δ, cuts in the $K\pi$ mass and in $z = E(D^*)/E_{beam}$ are applied to select the final sample of D* mesons. The angular distributions from HRS, JADE and TASSO are shown in fig. 19. The fitted asymmetries are listed in table V.

$c\bar{c}$					
Exp	$\sqrt{s}$ (GeV)	A (%) meas	$A_{expected}$	a_c	Method
MAC	29	-5 ± 11	-3	1.6 ± 3.6	c → μ
HRS	29	-25 ± 18	-9	2.6 ± 1.9	D*
AVERAGE	29			2.4 ± 1.7	
MARK J	34.6	-17 ± 9	-14	1.2 ± 0.6	c → μ
JADE	34.4	-27 ± 14	-14	1.9 ± 1.0	D*
TASSO	34.4	-13 ± 10	-14	0.9 ± 0.7	D*
AVERAGE	34.4			1.22 ± 0.4	
$b\bar{b}$				a_b	
MAC	29	-7 ± 9	-12	-0.6 ± 0.7	b → μ
MARK II	29			$-1.5 \pm ^{0.7}_{0.6}$	b → μ,e
AVERAGE	29			-1.1 ± 0.5	
MARK J	34.6	-15 ± 22	-25	-0.6 ± 0.9	b → μ
TASSO	34.4	-38 ± 28	-27	-1.4 ± 1.0	b → μ
JADE	34.4	-26 ± 9	-26	-1.0 ± 0.3	b → μ
AVERAGE	34.4			-0.99 ± 0.3	

Table V: Heavy Quark Asymmetries and Coupling Constants

9.3 Heavy Quark Coupling Constants

In table V, the results for asymmetries from inclusive lepton spectra and D* measurements are compiled; errors are statistical only. The coupling constants are derived by comparing the measured to the expected asymmetry and using $a_e = -1$, $Q_c = + 2/3$ and $Q_b = - 1/3$. Averaging over the data from PEP and PETRA which are shown in table V, $a_c = + 1.3 \pm 0.4$ and $a_b = - 1.0 \pm 0.3$ is obtained. The agreement between measurements and with the Standard Model predictions of +1 and -1 respectively is good (fig. 20).
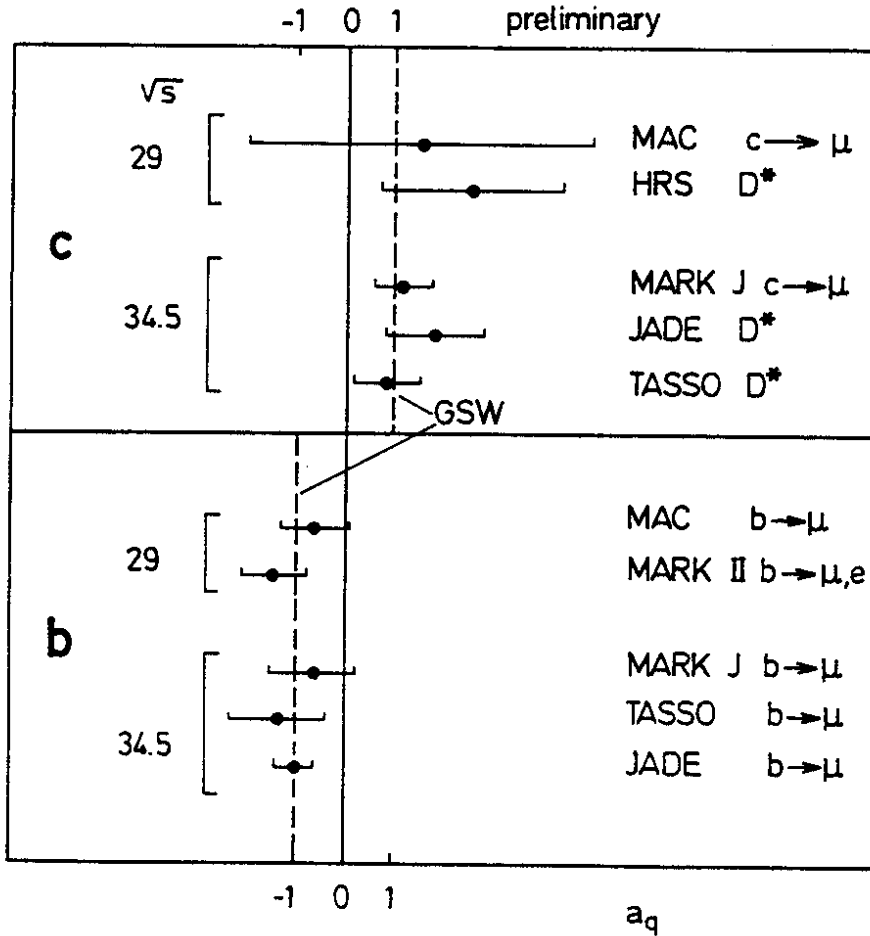
Fig. 20:   Coupling constants for c and b quarks from inclusive leptons
and D* analysis.

10. MEASUREMENT OF $\sigma(\nu_\mu e \rightarrow \nu_\mu e)$

A new neutrino experiment has come into operation at BNL. It is
operated by a BNL-Brown-KEK-Osaka-Pennsylvania-Stony Brook-Tokyo
collaboration[40]. The detector is constructed of planes of liquid
scintillator and proportional drift tubes. The average neutrino energy
is $<E_\nu> = 1.5$ GeV.

The data presented here originate from $8.8 \cdot 10^{18}$ protons on target
resulting in $\sim 10^6$ neutrino induced events. 316 of these events are
selected as candidates for the reaction $\nu_\mu e \rightarrow \nu_\mu e$ since they have an
electromagnetic shower in the fiducial volume of 75 tons. The pulse-
height distribution of these candidates in the scintillator and
proportional drift tubes (PDT) immediately downstream of a track or
event origin can be seen in fig. 21d. The other distributions in fig. 21
serve as control; they are from muons (a), electrons from e^-+p (b) and
photon induced events (c). The $\nu_\mu e$ candidates in 21d are a mixture of
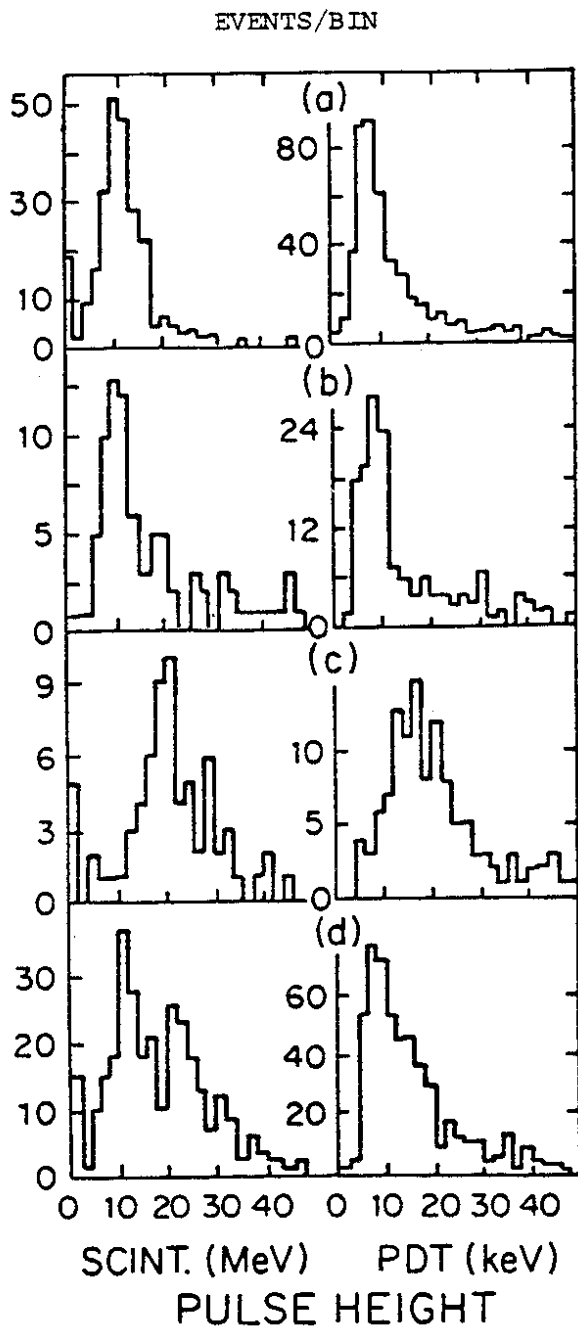all of these. Cuts are applied to single out minimum ionizing events.

EVENTS/BIN

SCINT. (MeV)   PDT (keV)

PULSE HEIGHT

Fig. 21: $\nu_\mu e$ scattering at BNL:
Pulseheight distributions in
scintillator and in the propor-
tional drift tubes (PDT) for (a)
identified muons; (b) electrons
from $\nu_e e \rightarrow e^- p$; (c) from $\gamma \rightarrow e^+ e^-$; (d)
ν events without muon and with an
electromagnetic shower (νe candidates).

The θ^2-distribution of this
minimum ionizing sample is
shown in fig. 22a where a clear
peak is observed at small θ^2.
The complementary sample (high
pulseheight in the scintillator
or PDT), shown in fig. 22b does
not show such a peak. The signal
attributed to $\nu_\mu e \rightarrow \nu_\mu e$ events is
51 ± 9 events over a background
of 25 ± 3 events. After efficiency
corrections and normalisation
to the charged current process
$\nu_\mu n \rightarrow \mu^- p$, the cross section is
obtained as:

$$\sigma(\nu_\mu e \rightarrow \nu_\mu e) =$$

$$(1.60\pm0.29\pm0.26) \cdot E_\nu(GeV) \cdot 10^{-42} cm^2$$

This result agrees well with
previous determinations of
σ_{ν_μ} [29,30]. A determination of the
electron coupling constants and
$\sin^2\theta_W$ will eventually be
possible when the analysis of
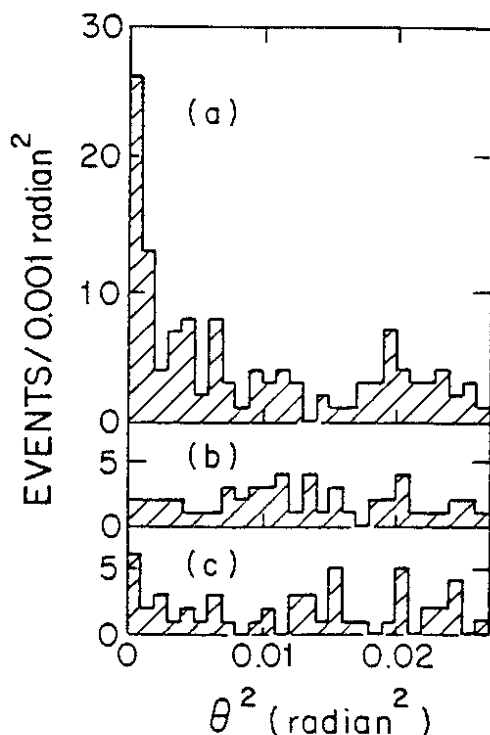antineutrino scattering has also
been completed.

Fig. 22:
θ^2 distributions for the $\nu_\mu e$ candidates: a) selecting the minimum ionizing sample in scintillator and PDTs; b) the complementary sample (high pulse-height in scintillator or PDTs); c) control sample: $\gamma \rightarrow e^+ e^-$.

36261

11. NEW RESULTS CONCERNING THE STRUCTURE OF CHARGED AND NEUTRAL CURRENTS

11.1 The CDHS collaboration has finalised their numbers for the cross section ratios of neutrino and antineutrino scattering on an (almost) isoscalar target (iron). The energy of the final hadronic shower was required to be greater than 10 GeV, the results are[41]:

$$R_\nu = \frac{\sigma(\nu_\mu N \rightarrow \nu_\mu X)}{\sigma(\nu_\mu N \rightarrow \mu^- X)} = 0.300 \pm 0.007$$

$$R_{\bar\nu} = \frac{\sigma(\bar\nu_\mu N \rightarrow \bar\nu_\mu X)}{\sigma(\bar\nu_\mu N \rightarrow \mu^+ X)} = 0.357 \pm 0.015$$

A new analysis to extract $\sin^2\theta_W$ is still under way. A preliminary value is $\sin^2\theta_W = 0.232 \pm 0.012$ including radiative corrections. The error contains statistical and experimental systematic errors. There is an additional theoretical uncertainty estimated to be nearly 0.01; the main contribution of which comes from uncertainties in the c-s transition matrix element.

11.2 The WA-25 collaboration at CERN did a simultaneous measurement of the left and right handed coupling constants of u and d quark[42]. They used the bubblechamber BEBC filled with deuterium in neutrino and antineutrino beams. The results are:

	measured	expected from GSW with $\sin^2\theta_W = 0.23$
u_L^2	0.13 ± 0.03	0.12
d_L^2	0.19 ± 0.03	0.18
u_R^2	0.02 ± 0.02	0.024
d_R^2	0.00 ± 0.02	0.006

11.3 The CHARM Collaboration measured the longitudinal muon polarisation in $\nabla_\mu N \rightarrow \mu^+ X$[43], which is sensitive to the Lorentz structure of the interaction. A limit of $\sigma_{S,P,T}/\sigma_{TOT} < 20\%$ was obtained at 95% confidence level. Assuming that there is no T contribution the limit for S and P contributions can be improved by using data at high inelasticity y only, which are more sensitive. Then one gets $\sigma_{S,P}/\sigma(TOT) < 7\%$, also at 95% confidence level.

11.4 Limits on Right Handed Currents

Two groups investigated the chiral structure of weak charged currents and gave mass limits for a possible right handed charged boson within the context of $SU(2)_L \times SU(2)_R \times U(1)$. In such theories the left and right handed charged bosons will mix to form mass eigenstates W_1 and W_2 with mixing angle ζ.

The decay of polarized muons was measured[44] by a Berkeley-Northwestern-TRIUMF collaboration. The 90% confidence level limit obtained on the mass of the right handed boson is $M(W_R) > 380$ GeV for any mixing angle ζ.

The CHARM collaboration[45] studied "inverse muon decay" in the CERN neutrino beam: $\nu_\mu e^- \rightarrow \nu_e \mu^-$. The limits obtained are $M_2/M_1 > 1.9$ and mixing angle $\zeta < 15^o$.

CONCLUSION

Electroweak interference has been established in different types of experiments over a large range of Q^2 and s from a few MeV^2 in atomic parity violation, through momentum transfers of 1 GeV^2 in polarized electron scattering and 100 GeV^2 in muon scattering to 1600 GeV^2 in e$^+$e$^-$ interactions. In this whole region all data are described well by the Standard Model, which has already been successful in describing neutrino scattering.

The quality of the data in e$^+$e$^-$ scattering has improved since they were first presented, mainly by increased statistics and data at higher energies. Tests of QED were improved and recently also measurements of processes of orders α^3 and α^4 have been carried out successfully. The averaged angular asymmetries for μ and τ pairs at the two cm energies of PEP and PETRA are:

$$\sqrt{s} = 29 \text{ GeV} \quad : \quad A_{\mu\mu} = -(6.3 \pm 0.9)\% ; \quad A_{\tau\tau} = -(3.6 \pm 2.1)\%$$

$$\sqrt{s} = 34.5 \text{ GeV} : \quad A_{\mu\mu} = -(10.8 \pm 1.1)\% ; \quad A_{\tau\tau} = -(7.6 \pm 1.9)\%$$

From the Standard Model one expects -6.3% and -9.4% at 29 and 34.5 GeV respectively with a theoretical uncertainty due to higher orders of 0.3% and 0.7% respectively.

The axial coupling constants derived from these asymmetries agree with e-μ-τ universality and also agree with previous determinations in neutrino scattering. For e and μ the errors are ~10%, whereas for the τ they are still ~25% and there is room for improvement. The propagator effect could be established by the PETRA μ pair data with more than 95% confidence. The limits derived for the mass of the Z^0 are in full agreement with recent measurements at the p$\bar{p}$ collider.

Determinations of heavy quark asymmetries are reported by almost all groups working at PEP and at PETRA. They start to give significant results, which agree well with Standard Model expectations, although the errors of many individual measurements are still large.

A new neutrino experiment is operating at BNL. It has given as a first result the cross section on $\nu_\mu e \to \nu_\mu e$, which agrees with previous determinations. There is now a world wide total of ~250 neutral current events from $\nu_\mu e$ and $\bar{\nu}_\mu e$.

New results on the structure of charged weak currents confirm their V-A structure. The limit on the mass of a right handed intermediate charged boson in left-right symmetric theories has been increased to > 350 GeV.

REFERENCES

1. S.L. Glashow, Nucl. Phys. 22 (1961) 579; Rev. Mod. Phys. 52 (1980)539;
   A. Salam, Phys.Rev. 127 (1962) 331; Rev.Mod.Phys. 52 (1980) 525;
   S. Weinberg, Phys.Rev.Lett. 19 (1967) 1264; Rev.Mod.Phys. 52 (1980)515.
2. C. Prescott et al., Phys. Lett. 77B (1978) 347 and 84B (1979) 524.
3. A recent review of atomic physics experiments was given by
   M. Davier in Paris Conf.*, page C3-471 and references therein.
4. M.A. Bouchiat et al., Phys. Lett. 117B (1982) 358.
5. C. Bouchiat and C.A. Piketty, Preprint Paris LTPENS 83/18 and C-197.
6. BCDMS Coll., A. Argento et al., Phys. Lett. 120B (1983) 245.
7. Particle Data Group, Phys. Lett. 111B (1982).
8. UA1 Coll., G. Arnison et al., Phys. Lett. 126B (1983) 398
   and contribution to this conference by B. Sadoulet;
   UA2 Coll. CERN preprint CERN-EP/83-112
   and contribution to this conference by A. Clark.
9. R. Budny, Phys. Lett. 55B (1975) 227.
10. CELLO Coll., H.-J. Behrend et al., Z. Phys. C16 (1983) 301.
11. JADE Coll., W. Bartel et al., Z. Phys. C19 (1983) 197.
12. MARK J Coll., A. Boehm in Erice Study Conf.*
13. TASSO Coll., DESY preprint 83-089 (1983) to be published in
    Z. Phys.
14. MARK II Coll., M.E. Levi et al., SLAC-PUB-3177 (1983).
15. MAC Coll., G. Goldhaber in XVIIIth Rencontre de Moriond on
    Electroweak Interactions, March 1983, to be published.
16. HRS Coll., S. Ahlen et al., C-156.
17. F.A. Berends et al., Nucl. Phys. B68 (1973) 541;
    F.A. Berends and Komen, Phys. Lett. B63 (1973) 432.
18. F.A. Berends et al., Nucl. Phys. B63 (1973) 381;
    F.A. Berends et al., Nucl. Phys. B177 (1981) 237;
    F.A. Berends and R. Kleiss, DESY-Report 80-66 (1980).
19. F.A. Berends, R. Kleiss and S. Jadach, Nucl. Phys. B202 (1982) 63.
20. MAC Coll., W.T. Ford et al., Phys. Rev. Lett. 51 (1983) 257 and
    private communication.
21. Z.J. Rek and I. Schmitt did the computation for the MAC group;
    a similar program is described in F. Gutbrod and Z.J. Rek,
    Z. Phys. C1 (1979) 171.
22. CELLO Coll., H.-J. Behrend et al., Z. Phys. C14 (1982) 283;
    JADE Coll., W. Bartel et al., Phys. Lett. 108B (1982) 140;
    MARK J Coll., B. Adeva et al., Phys. Rev. Lett. 48 (1982) 1701;
    TASSO Coll., R. Brandelik et al., Phys. Lett. 110B (1982) 173.
23 - 26 see also: J. Salicio, P. Grosse-Wiesmann, B. Naroska,
    G. Mikenberg, G. Chadwick, H. Ogren in Erice Study Conf.*
23. PLUTO Coll., Ch. Berger et al., DESY preprint 83-84 (1983),
    to be published in Z. Phys. C;
    TASSO Coll., see ref. 13;
    MARK J Coll., G. Herten and A. Boehm in Brighton Conf.*;
    JADE Coll., A. Ball, Brighton Conf.* and private communication.
24. MAC Coll., E. Fernandez et al., Phys. Rev. Lett. 50 (1983) 1238;
    MAC Coll., E. Fernandez et al., SLAC-PUB-3133 (1983) C-78.

25. CELLO Coll., H.-J. Behrend et al., Phys. Lett. 114B (1982) 292;
    JADE Coll., private communication;
    TASSO Coll., private communication;
    MARK J Coll., G. Herten and A. Boehm in Brighton Conf.*
26. MAC Coll., D.M. Ritson in Paris Conf., page C3-52.
27. G. Passarino and M. Veltman, Nucl. Phys. B160 (1979) 151;
    G. Passarino, Nucl. Phys. B204 (1982) 237;
    M. Böhm and W. Hollik, Nucl. Phys. B204 (1982) 45, DESY 83-060;
    W. Hollik in Conf. on Radiative Corrections in SU(2) x U(1),
    June 1983, Trieste, Italy, to be published.
    M. Greco et al., Nucl. Phys. B171 (1979) 118; B197 (1982) 543;
    S. Bellucci, Higher Order Corrections to the Muon Backward-
    Forward Asymmetry, in Conf. on Radiative Corrections, June 1983,
    Trieste, Italy, to be published.
    R. Decker, E.A. Paschos, R.W. Brown, Un. Dortmund preprint
    DO-TH 83/16;
    W. Wetzel, Un. Heidelberg preprint, May 1983.
28. W. Krenz, Un. Aachen preprint PITHA 82/26.
29. CHARM Coll., F. Bergsma et al., Phys. Lett. 117B (1982) 272.
30. R.H. Heisterberg et al., Phys. Rev. Lett. 44 (1979) 635.
31. CELLO Coll., H.J. Behrend et al., Z. Phys. C16 (1983) 301;
    JADE Coll., W. Bartel et al., Phys. Lett. 99B (1981) 281;
    MARK J Coll., D.P. Barber et al., Phys. Rev. Lett. 46 (1981) 1663
    TASSO Coll., R. Brandelik et al., Phys. Lett. B117 (1982) 365;
    A. Boehm in Brighton Conf.*, K. Winter in Erice Study Conf.*
32. J.E. Kim et al., Rev. Mod. Phys. 53 (1981) 211.
33. MARK I Coll., T. Himel et al., Phys. Rev. Lett. 41 (1978) 449.
34. MARK II Coll., M.E. Nelson et al., Phys. Rev. Lett. 50 (1983) 1542
    and SLAC-PUB--3059 (1983) and private communication.
35. MARK J Coll., B. Adeva et al., Phys. Rev. Lett. 51 (1983) 443 and
    private communication;
    JADE and TASSO Coll., private communication.
36. CELLO Coll., H.J. Behrend et al., Z. Phys. C19 (1983) 291 and C-221.
37. A. Ali, Z. Phys. C1 (1979) 25;
    M.J. Puhala et al., Phys. Rev. D25 (1982) 95 and 695.
38. J. Jersak et al., Phys. Lett. 98B (1981) 363.
39. HRS Coll., S. Ahlen et al., C-157 and private communication;
    JADE Coll., private communication;
    TASSO Coll., M. Althoff et al., Phys. Lett. 126 B (1983) 493
    and private communication.
40. L.A. Ahrens et al., Phys. Rev. Lett. 51 (1983) 1514.
41. CDHS Coll., Ch. Geweniger in Erice Study Conf.* and Brighton Conf.*
42. D. Allasia et al., (WA 25) Amsterdam preprint, NIKHEF-H/83-12,
    submitted for publication.
43. CHARM Coll., M. Jonker et al., C-86, CERN-EP/82-207 (1982),
    to be published in Z. Phys. C.
44. J. Carr et al., C-107; a more detailed discussion of this
    experiment will be given in S. Yamada's review in this conference.
45. CHARM Coll., F. Bergsma et al., C-84, CERN EP/82-206 (1982),
    to be published in Phys. Lett.

*   <u>Brighton Conf.</u>: Proc. of the Int. Europhysics Conf. on High
Energy Physics, Brighton, U.K., July 1983; to be published.

<u>Paris Conf.</u>: 21st International Conference on High Energy
Physics, Paris 1983; Les Editions de Physique, France.

<u>Erice Study Conf.</u>: Europhysics Conference on Electroweak
Effects at High Energy, Erice 1982; to be published.

DISCUSSION

S.F. Tuan, University of Hawai: I understand that you derive from e^+e^- a mass of the Z^0 of 76 GeV, whereas UA1 and UA2 find masses around 95 GeV as we heard yesterday. Isn't this a surprise?
Answer: It is not, if you take into account the errors. The 95% confidence limits from e^+e^- scattering are $60 < M_Z < 170$ GeV. Unfortunately e^+e^- isn't very sensitive to the mass of the Z^0.

J. Haissinski, Saclay: I would just like to mention that in a paper submitted to this conference (#222), the CELLO group has attempted to look at the τ polarlization by looking at the momentum distribution of the decay leptons in the laboratory. This will then give you the parity violating coupling constants g_{VA}.
Answer: This is indeed a very interesting prospect in the τ analysis and should be attempted further. Unfortunately polarizations are only of the order of 1%. So you need good momentum resolution and good statistics. Maybe detectors like HRS could do that, given enough statistics.

G. Wolf, DESY: Could you comment on the limit on the right handed current obtained from decay of polarized muons? This limit probably depends on the mass of the neutrino. What happens if m_ν is not 0?
M. Strovink: The TRIUMF experiment is sensitive for right handed ν masses below ~ 5 to 10 MeV.

W. Panofsky, SLAC: In the uncertainty of $\sin^2\theta_W$ derived in neutrino scattering, was the nuclear effect taken into account, particularly considering the EMC effect?
Answer: Nuclear effects are taken into account. But I am told by the authors that the EMC effect is not a problem, because they take their own structure functions, measured on the nucleus which they also use for the determination of $\sin^2\theta_W$.

Boris Kayser, National Science Foundation: You used the Reines electron neutrino experiment as part of narrowing down the ambiguities in determining coupling constants. But there is only this one experiment. Do you know of any plans to repeat it anywhere?
Answer: No, I don't. But the unique solution does not only depend on the Reines data. If you are willing to assume factorization, which I did all the time, by the way, and think you can trust the handling of nuclear effects, then the eD and μD experiments can also be used.